

UNIVERSITY OF CALIFORNIA

Los Angeles

Locating the *Sry* transgene and measuring estrous cycles in rats with manipulations of the testis-determining factor *Sry*

A thesis submitted in partial satisfaction of the requirements
for the degree Master of Science in Physiological Science

by

Helen Ruth Schmidtke

2024

© Copyright by

Helen Ruth Schmidtke

2024

ABSTRACT OF THE THESIS

Locating the *Sry* transgene and measuring estrous cycles in rats with manipulations of the testis-determining gene *Sry*

by

Helen Ruth Schmidtke

Master of Science in Physiological Science

University of California, Los Angeles, 2024

Professor Arthur P. Arnold, Chair

The Four Core Genotypes (FCG) transgenic mouse model allows us to investigate if an observed sex difference in phenotype is caused by gonadal hormones, sex chromosome effects, or both¹. The FCG model currently exists in mice only, limiting generalizability across species. Not only does developing an FCG model in rats improve the applicability of the results, but rats have advantages as a model organism when studying neurodevelopmental, cardiovascular, and substance use disorders due to their larger size and docile nature. To make rats like FCG mice, the region of the Y chromosome harboring *Sry*, the testis-determining gene was mutated (producing the Y^Δ chromosome), reducing the number of *Sry* genes and preventing testis development. In addition, a bacterial artificial chromosome (BAC) encoding *Sry* was inserted as a transgene in an autosome in several transgenic rat lines, producing XX rats with testes. One goal of the present study was to locate the insertion point of the *Sry* transgene. Using a

commercially available Y Chromosome paint, and a fluorescently labeled *Sry* transgene probe, we performed metaphase fluorescent in-situ hybridization (FISH), to locate the transgene inserted in Chromosome 11 in transgenic line 208, Chromosome 20 in line 424, and Chromosome 2 in line 733. We also compared estrous cycling of gonadal females with different sex chromosome complements, as a bioassay for complex endocrine regulatory mechanisms regulating ovulation and estrus. We compared XX or XXY^{Δ} sex chromosomes, by observing the type and concentration of cells collected in daily vaginal swabs of both groups. This experiment revealed no difference in estrous cycle length between gonadal females with or without a Y^{Δ} chromosome, therefore uncovering no effect of sex chromosome complement on factors controlling estrus.

The thesis of Helen Ruth Schmidtke is approved.

Stephanie Correa Van Veen

Barnett Schlinger

Arthur P. Arnold, Committee Chair

University of California, Los Angeles

2024

Acknowledgments

I'm deeply grateful to my mentor and the chair of my committee, Dr. Art Arnold, for the opportunity to pursue my thesis project in the Arnold Lab. His expertise and guidance were instrumental both in completing this thesis and in my growth as a scientist and researcher. I'm also grateful to my committee members, Dr. Stephanie Correa and Dr. Barney Schlinger, for their insight and feedback throughout my project timeline.

I want to thank the Arnold Lab's Associate Project Scientist, Xuqi Chen, for her invaluable help, patience, and mentorship while I learned the techniques required for my project. Many thanks are also necessary to our lab manager, Haley Hrcir, without whom I would not have the materials to complete my project.

Lastly, I thank my friends, family, and significant other for their unending support. Between proofreading my papers, bringing me dinner while I worked late, and listening to me rant when my experiments didn't go as planned, they were a magnificent support system. I'm so grateful to have them by my side throughout this journey.

TABLE OF CONTENTS

Abstract	ii
Committee Page	iv
Acknowledgments	v
Table of Contents	vi
List of Tables and Figures	vii
List of Abbreviations	viii
List of Symbols	x
Introduction	1
Materials and Methods	9
Results	15
Discussion	22
Conclusion	27
Figures	28
Tables	42
References	46

LIST OF TABLES AND FIGURES

Figure 1	28
Figure 2	29
Figure 3	30
Figure 4	31
Figure 5	32
Figure 6	33
Figure 7	34
Figure 8	35
Figure 9	36
Figure 10	37
Figure 11	38
Figure 12	39
Figure 13	40
Figure 14	41
Table 1	42
Table 2	43
Table 3	44
Table 4	45

LIST OF ABBREVIATIONS

ARC	Animal Research Committee
BAC	Bacterial Artificial Chromosome
BSA	Bovine Serum Albumin
cDNA	Complementary Deoxyribonucleic Acid
CG%	Percentage of Cytosine and Guanine Content
DAPI	4',6-diamidino-2-phenylindole
DLAM	Department of Laboratory Animal Medicine
DMEM	Dulbecco's modified Eagle's Medium
DNA	Deoxyribonucleic Acid
EDTA	Ethylenediaminetetraacetic acid
FBS	Fetal Bovine Serum
FCG	Four Core Genotypes
FISH	Fluorescent <i>In Situ</i> Hybridization
HPG	Hypothalamic-Pituitary-Gonadal
KCl	Potassium Chloride
KO	Knockout
MCW	Medical College of Wisconsin
MIH	Müllerian Inhibiting Hormone
MSCI	Meiotic Sex Chromosome Inactivation
P# (i.e. P2)	Postnatal Day # (i.e. Postnatal Day 2)
PAR	Pseudoautosomal Region

PBS	Phosphate Buffered Saline
PCR	Polymerase Chain Reaction
rtPCR	Reverse Transcription Polymerase Chain Reaction
SD	Sprague Dawley
<i>Sry</i>	Sex-Determining Region of the Y Chromosome
<i>Sry</i> Box	Sex-Determining Region of the Y Chromosome Box
<i>Sry</i> TG+	Possesses the <i>Sry</i> transgene
SSC	Sodium Citrate
<i>Tdf</i>	Testis-Determining Factor
<i>Tdf-KO</i>	Testis-Determining Factor Knockout
UCLA	University of California, Los Angeles
WT	Wild-Type
XXF	XX gonadal females
XXM	XX gonadal males
XXTG	XX transgenic gonadal male
XYF	XY gonadal females
XYM	XY gonadal males

LIST OF SYMBOLS

Δ	As in Y^Δ , denotes the deletion of the target <i>Sry genes</i> from the endogenous rat Y Chromosome
-	As in Y^- , denotes the deletion of the target <i>Sry</i> gene from the endogenous mouse Y Chromosome
°	Degrees, as in degrees Celsius or °C

INTRODUCTION

Between 2.0 and 1.3 billion years ago, eukaryotic organisms evolved to reproduce sexually (Otto, 2008). Prior to this point reproduction was asexual, in which a parent organism produces a genetically identical daughter organism (Tabata et al., 2016). The first sexually reproductive species were isogamous, meaning their gametes were equal in size between both parent organisms (Togashi et al., 2012). Anisogamy, on the other hand, refers to sexual reproduction between gametes of differing sizes; it is thought to have evolved from isogamy and today is the most common form of sexual reproduction (Togashi et al., 2012). The evolution of anisogamous reproduction is substantial because it is thought to be the first instance of sexual dimorphism, that is a significant difference in traits between males and females of the same species, in the phylogenetic tree (Cyrus Chu & Lee, 2012).

As the progenitor species of anisogamy evolved and became more complex, so did their means of producing anisogamous gametes. Males and females developed radically different reproductive systems with their own unique physiologies. One of the most substantial differences between males and females is in the secretion of gonadal hormones. Sexual differentiation theory suggests that the difference in hormone secretions from the gonads between males and females of the same species give rise to sexually dimorphic phenotypes (Arnold, 2017).

Frank Lillie (1939) stated that sex chromosomes (“zygotic sex”) dictates gonadal sex, which in turn cause sexual differentiation of non-gonadal traits, (Arnold, 2017). Lillie first proposed this idea based on his observations of the freemartin effect, wherein genetically female calves undergo masculinization and become intersex when in utero with a genetically male twin. He believed this was caused by the presence of substances in the blood with masculinizing or feminizing effects. Alfred Jost built upon these findings in his research, where he removed the

gonads of rabbits prenatally before returning them to the womb (Jost, 1970). He found that prenatal castration caused the development of internal and external female genitalia and the regression of internal male genitalia neonatally; alternatively, prenatal ovariectomy did not affect gonadal development in females. Furthermore, internal and external male genitalia appeared in genetic females when exposed to a graft of testis tissue. Females treated with testosterone prenatally developed masculine external genitalia but retained Müllerian Duct derivatives such as the uterus. From these findings, Jost suggested that masculinization is promoted by two testicular hormones: testosterone, which stimulates the growth of internal male genitalia, and Müllerian Inhibiting Hormone (MIH), which prevents the development of internal female genitalia (Jost, 1970). Experiments critical to sexual differentiation theory were those of Phoenix et al., in which pre- and postnatal administration of testosterone to females permanently affected phenotype and development. In contrast, administration in adulthood produced temporary and reversible effects (Phoenix et al., 1959). Altogether, these studies present sex determination involving differentiation of the gonads, leading to sexual differentiation caused by gonadal hormones, and highlight the presence of critical periods where hormones can vastly influence sexually dimorphic phenotypes.

Lillie's understanding of hormones and sex determination was ahead of his time and was the basis for foundational studies in neuroendocrine and reproductive research. However, he did not perform karyotype analysis to determine the chromosomal sex and instead inferred it based on whether the calves possessed ovaries or testes. While it's obvious from the work of Lillie, Jost, and Phoenix et al. that hormone exposure during specific developmental stages is instrumental in the development of primary and secondary sexual characteristics, genetic sex differences were present long before the evolution of hormones and the gonads (Otto, 2008).

The first theories of sex determination date back to the early Classical period in Greece and cite the position of the fetus in the womb, the sperm's origin from the left or right testicle, and the temperature of the womb during conception as sources of biological sex (Piprek, 2020). Scientific evidence for sex determination, however, did not follow until the late nineteenth century and was spurred by the discovery of chromosomes in 1888 (Waldayer, 1888).

In 1891, Hermann Henking sought the mechanisms of meiotic division in the sperm of *Hemiptera* (1891). During this research, he observed the nuclei of some sperm had eleven chromosomes while others had twelve. The twelfth chromosome, which Henking coined "element X", behaved differently from the other chromosomes in anaphase I & II (Paliulis et al., 2023). This was supported by American zoologist Clarence McClung, who first proposed that element X, or the "accessory chromosome", is sex-determining (McClung, 1899). This was confirmed by Nettie Stevens in her 1905 observations of mealworms, where she noted that female cells possess 20 chromosomes of equal size while male cells have 19 equally sized chromosomes plus 1 much smaller chromosome (Stevens, 1905).

In 1914, Calvin Bridges proposed sex determination in *Drosophila melanogaster* was controlled by the number of X Chromosomes (Bridges, 1914). However, it was not until 1959 that Charles Ford concluded from his observations of Turner's Syndrome in humans that the number of Y Chromosomes dictated sex determination. Additionally, he proposed that the Y Chromosome contained a segment causing testis development, which he called testis-determining factor (TDF). Subsequent research in the genetic basis of sex sought identification of the specific Y Chromosome genes responsible for testis development; however, limitations in genetic technology stalled progress. The boundaries of the TDF region were narrowed over time using complementary DNA (cDNA) fragment comparison between the X and Y Chromosomes

(Palmer et al., 1990). This was until 1990, when Andrew Sinclair examined the genomes of several patients who were genetically female but possessed male gonads and masculine secondary sex characteristics (Sinclair et al. 1990). By comparing each of their genomes to Y-unique sequences and mapping any overlapping sequences within the group, he identified a 35 kb sequence shared among each of these individuals, which he deemed the sex-determining region of the Y Chromosome (*Sry*). The *Sry* gene encodes the SRY protein, which was subsequently proven to cause the development of testes in mice (Goodfellow & Lovell-Badge, 1993)

These findings were instrumental in the rethinking of sexual differentiation theory (McCarthy & Arnold, 2011). In addition to the twentieth-century understanding that sex determination leads to sexual differentiation, the idea arose that the sex chromosomes could directly affect sexual differentiation in non-gonadal tissues because of their differing gene content (Arnold, 2012). This led to a new theory in the field of sexual differentiation: sexually dimorphic phenotypes could stem from the sex chromosomes or through gonadal hormones (Fig. 1). The issue with this theory is that it is difficult to test, since wild-type XY mammals develop testes and wild-type XX mammals develop ovaries.

Enter the Four Core Genotypes (FCG) model, which was first developed in the 1990s through the works of Lovell-Badge and Robertson (1990) as well as Burgoyne et al. (1998) (Arnold & Chen, 2009). Lovell-Badge and Robertson had discovered an XY mouse with ovaries, which possesses a mutation in which the testis-determining gene *Sry* was deleted from the Y chromosome; this resulted in a Y chromosome that was no longer testis-determining (Y^-) and produced gonadal females. Moreover, adding the *Sry* gene back to an autosome of an XY^- mouse was accomplished by Burgoyne et al., which created XY^- mice that have male gonads (XY^-

Sry⁺) and father mice with four genotypes. The four kinds of animals in the FCG mouse model are XX gonadal females (XXF), XX gonadal males (XXM), XY gonadal females (XYF), and XY gonadal males (XYM). These four form a two-way ANOVA test to study hormonal versus sex chromosome effects: sex differences observed in FCG animals with the same sex chromosome complement but different gonads are attributed to differences in gonadal hormones. Alternatively, when sex differences are present in FCG animals with the same gonads but different sex chromosomes, the observed difference is a sex chromosome effect.

Two alterations to the genome are required to make FCG animals. The first is the deletion of the sex-determining region of the Y Chromosome (*Sry*). *Sry* regulates the development of testes by producing the SRY protein. The testes then secrete testosterone and AMH which cause sexual differentiation of the external and internal male genitalia plus many male-typical phenotypes in non-gonadal tissues (CITE). Removing the *Sry* gene from the Y chromosome blocks testis development and creates XYF animals. This new Y Chromosome lacking *Sry* is denoted as the Y minus (Y⁻) Chromosome in the FCG mouse model. The second change is the insertion of *Sry* onto an autosomal chromosome. Insertion of *Sry* onto an autosome allows for testis development independent of inheriting a Y Chromosome. Transgenic gonadal males (XY⁻*Sry*⁺), also known as “true Four Core fathers”, possess a Y Chromosome without *Sry* but inherited *Sry* on an autosome.

We have generated a rat *Sry*-manipulated model using similar genetic alterations. The purpose of generating a *Sry*-manipulated model in rats is twofold: generalizability of findings and improved experimental technique. The FCG mouse model was instrumental in our understanding of sex differences in autoimmunity (Golden et al., 2019; Itoh et al., 2019; Ghosh et al., 2021; Doss et al., 2021), metabolism (Chen et al., 2012; Chen et al., 2013; Link et al.,

2013; Chen et al., 2015; Link et al., 2017; Zore et al., 2018), and cardiovascular function (Li et al., 2014; Dadam et al., 2017; Ensor et al., 2021; Wiese et al., 2022), as well as behaviors related to substance abuse (Sneddon et al., 2022; Sneddon et al., 2023), mood regulation (Seney et al., 2013; Puralewski et al., 2016; Barko et al., 2019), and nociception (Gioiosa et al., 2008; Taylor et al., 2022). However, without another model organism to study, the findings generated by studying the mouse model are specific only to mice. Rats are also more beneficial in neuroscience because their brains are larger and they are more docile animals than mice.

Although the mouse FCG model and rat *Sry*-manipulated model were both produced by deletion of the endogenous *Sry* and insertion of the *Sry* transgene onto an autosome, the two models have significant differences. The genotypes produced in the FCG mouse model are XX gonadal females, XX gonadal males, XY gonadal females, and XY gonadal males (Arnold & Chen, 2009; Burgoyne & Arnold, 2016). In the rat model, the modified Y chromosome (Y^Δ) could not be combined in the same animal with the *Sry* transgene, because genetic manipulation of producing the Y^Δ chromosome also deleted genes required for spermatogenesis. Thus, the Y^Δ chromosome must be passed to the new generation from XY^Δ mothers. This creates a problem because XY^Δ mothers produce three kinds of eggs, X, Y, and XY^Δ . Thus, XY^Δ mothers mated to WT XY fathers produce three types of gonadal females: XX, XXY^Δ , and a small number of XY^Δ females. Because the initial breeding of XY^Δ females in our lab failed to discriminate the two types of females bearing the Y^Δ chromosome, the XY^Δ group was lost as the XXY^Δ genotype became more predominant. XXY^Δ females produce two types of egg cells, X and XY^Δ , and therefore produce no XY^Δ female offspring. One goal of the present project was to compare the estrous cycling of the two types of females now available in our lab, XX and XXY^Δ .

This non-Mendelian inheritance could stem from the differential behavior of X and Y chromosomes in sperm and egg cells during meiosis (Turner et al., 2000). In XX primary oocytes, the X Chromosomes pair during Prophase I like autosomes. In XY primary spermatocytes, the X and Y chromosomes pair at the Pseudoautosomal Region (PAR) of both chromosomes, which is a region of shared genes between the X and Y Chromosomes and is the only location where these chromosomes recombine (Arnold, 2023). Once the X and Y Chromosomes are paired at their PARs, they become encased in a specialized chromatin area called the XY body or sex body. The XY body prevents transcription and silences the sex chromosomes until the end of prophase; this process is known as meiotic sex chromosome inactivation (MSCI) (Van Der Heijden et al., 2011).

The XY^Δ primary oocytes of gonadal females, however, do not form the XY body during Prophase I. This is because egg cells typically possess two X Chromosomes and therefore did not evolve this adaptation. As a result, the sex chromosomes remain unpaired in the cytoplasm and XY^Δ females can produce X eggs, Y^Δ eggs, and XY^Δ eggs. In the primary oocytes of XX^{YΔ} females, the two X Chromosomes pair as seen in XX eggs. This leaves the Y^Δ Chromosome by itself in the nucleus and free to move into either of the daughter cells. However, since both daughter cells will contain an X Chromosome, XX^{YΔ} females can only produce two kinds of eggs: X eggs and XY^Δ eggs.

The *Sry*-manipulated rats that we have produced allow numerous interesting comparisons. First, comparing the estrous cycles of XX and XX^{YΔ} gonadal females represents one approach to detecting how possessing the Y^Δ Chromosome affects the HPG axis function in females with 2 X Chromosomes. In addition, this comparison reveals how sex chromosome trisomy influences the HPG axis in gonadal females. Finally, studying XX^{YΔ} could eventually

(not in this thesis) give insight into the effects of a Klinefelter's Syndrome-like genotype. Klinefelter's Syndrome occurs in human gonadal males (XXY) and affects physical traits (Plotton et al., 2010; Simpson et al., 2003; Smyth & Bremner, 1998), learning abilities (Visootsak & Graham, 2009), and behavior (Ratcliffe, 1999). While the Klinefelter's-like rats in our model are gonadal females (XXY Δ), these rats can be used to examine behavioral phenotypes present in Klinefelter's, such as difficulty with social adjustment and regulating aggressive behavior (Ratcliffe et al., 1982; Visootsak & Graham, 2009).

Another facet of the rat *Sry*-manipulated model that must be considered before experimental use is the location of the *Sry* transgene in the transgenic males. XX transgenic males were made by pronuclear injection of transgenic DNA into XX zygotes. However, this method leads to the insertion of the transgene into a random location of the genome. Pinpointing the location of insertion is crucial to creating the model with the least confounding variables. If the transgene is inserted in the middle of a crucial gene or gene family, it could disrupt processes related to the regulation of these interrupted genes, which would then represent a confound for gonadal effects when comparing groups with or without the transgene. To increase our odds of the transgene being inserted into a non-coding region within the genome, we have three lines of FCG rats: 208, 424, and 733. Therefore, the second goal of this project was to locate the insertion point of the *Sry* transgene in each line using karyotyping, metaphase FISH, a commercially available Y Chromosome paint, and a BAC *Sry* probe.

MATERIALS AND METHODS

Animal Care

XX gonadal males were generated by pronuclear injection of the BAC clone RNECO-180E22, containing the *Sry1*, *Sry3C*, and *Sry4A* genes, into rat zygotes. Although the first injections and this approach were validated at the Medical College of Wisconsin (MCW), the lines studied here were produced by the Transgenic Animal Core of the University of Michigan (Arnold et al., 2023). Of the 22 rats generated carrying the transgene, four were XY gonadal males with the transgene that sired XX gonadal male offspring. These four lines of XY transgenic founders are 208, 424, 733, and 737. All four were backcrossed to the Sprague Dawley Crl:CD (SD) strain code 001 (Charles River, Wilmington, MA). XY gonadal females were generated by pronuclear injection CRISPR-Cas9 guide RNAs targeting a region of the Y chromosome encoding several *Sry* genes, in of Sprague Dawley Crl:SD stain code 400 (Charles River Laboratories). One gonadal female with the Y^{Δ} Chromosome was fertile and passed the Y^{Δ} to their offspring when bred with an XY wild-type male. All rats were backcrossed to Sprague Dawley CD (001) for 9-14 generations prior to experiments.

The genotypes produced in the *Sry*-manipulated rat model arise from two crosses. First, breeding an XX wild-type female with an XY(*Sry*TG+) animal produces wild-type gonadal females (XXF), wild-type gonadal males (XYM), XX transgenic males (XXM) and XY males with the *Sry* transgene (XYM(*Sry*TG+)) (Arnold et al., 2023). Second, breeding an XY^{Δ} or XXY^{Δ} female with a wild-type XY male produces wild-type gonadal females (XXF), wild-type gonadal males (XYM), XY^{Δ} females (XYF), XXY^{Δ} females (XXYF), and XY^{Δ} males (XYYM), except that breeding of XXY^{Δ} females does not produce XY^{Δ} daughters.

All experimentation was carried out at the University of California, Los Angeles. Rats were maintained on a 12:12 light-dark cycle, and all samples were collected during the light stage. Protocols were approved by the UCLA Chancellor's Animal Research Committee (ARC).

Genotyping PCR

All animals in this project were genotyped via polymerase chain reaction (PCR) beginning at postnatal day 2 (P2). Tissue from the tail was collected in a 1.5mL Eppendorf tube. Chelex was added to the sample and incubated on a hot block at 95°C for 45 minutes to isolate the DNA. During DNA extraction, the PCR master mix was made using water, Taq polymerase, and primer. The primers for Med14 assayed the presence of the Y Chromosome and the X chromosome, and the primer set 180E22.1 detected the presence of the *Sry* transgene. After PCR, samples were loaded into a 2% agarose gel with GelRed Nucleic Acid Stain 10,000X in water (Cat #41003) and run for 25 minutes at 100V. Afterward, the gel was visualized with the Kodak Electrophoresis Documentation and Analysis System 120 and a FOTO/UV 26 machine and was photographed using an iPhone camera.

Estrous Cycle Analysis

XX and XXY^Δ gonadal female siblings were compared at approximately 2 months old. Vaginal smears were collected and staged at the same time daily, between 10-11 AM, for 21 days to maintain a regular 24-hour interval between smears. Cotton swabs were dipped in 1X PBS immediately before smear collection to maximize the yield of cells. The estrous cycle stage of each vaginal smear was determined under a light microscope according to the estrous

cycle stage criteria described by Cora et al (2015). One full estrous cycle was calculated as the number in whole days between estrus stages.

Tail Tip Fibroblast Cultures

Fibroblast cultures were prepared using the procedure of Yuichiro Itoh (personal communication, 2023). One millimeter of live tissue from the ear or tail was collected from rats in the 208, 424, and 733 lines. The sample was sanitized with 70% ethanol, placed in a 1.5mL Eppendorf tube containing 1X PBS, and minced inside of the tube using scissors cleaned with 70% ethanol. The tissue was then transferred to a conical tube containing 100 μ L of 0.25% trypsin-1mM ethylenediaminetetraacetic acid (EDTA) and incubated at 37°C for 1-2 hours to digest the tissue piece. The tube was flicked intermittently throughout this time to assist in digestion. After digestion, the conical tube containing the sample was brought to the culture room hood. Here, a serological pipet was used to transfer 5mL Advanced Dulbecco's modified Eagle's medium (DMEM) solution with 5% fetal bovine serum (FBS), 1% pen/strep, 1% Glutamax (Cat# 35050-061), and 0.5% Amphotericin B to the conical tube. The tissue was pipetted up and down 10-20 times. The cell suspension was then transferred to a 60mm tissue culture dish and incubated at 37°C in 5% CO₂ until cells were 50-70% confluent.

Metaphase Preparation

This protocol was adapted from the procedure of Yuichiro Itoh (personal communication, 2023). When cultures were 50-70% confluent, 10 μ L of [μ g/mL] Colcemid was added per 1 mL of media in the dish (so 50 μ L for 5mL media) and incubated at 37°C in 5% CO₂ to stop cell division and inhibit spindle formation. After 2-4 hours, the medium was removed, and cells were

washed twice with 1X PBS. 400 μ L of 0.25% trypsin-1mM EDTA was added to the dish and incubated at 37°C in 5% CO₂ to detach the cells from the bottom of the dish. Once cells are detached, 5mL media was added to the dish and pipetted up and down 10-20 times. This cell suspension was transferred to a 15mL conical tube. The empty dish was viewed with an inverted microscope to confirm that all cells were transferred from the dish to the conical tube.

The samples were centrifuged at 500g for 5 minutes to concentrate cells into a pellet at the bottom of the tube. The supernatant was aspirated until there was 2mL left, and then the cell pellet was thoroughly resuspended by flicking the tube. 10mL of the hypertonic solution 0.075M KCl was added stepwise to the suspension to make the cells swell. After letting this solution sit at room temperature for 15 minutes, 10 drops of a room temperature solution of methanoic acid (3:1 methanol to acetic acid) were added to the sample. The samples were again centrifuged at 500g for 5 minutes and aspirated until 2mL solution remained in the tube. The cell pellet was then resuspended by inverting to prevent bursting the fragile swollen cells.

After resuspension, 5mL of ice-cold methanoic acid was added stepwise to the tube and left on ice for 15 minutes. The samples were then inverted and centrifuged at 500g for 5 minutes. The supernatant was aspirated until there was 2mL left, then the cell pellet was resuspended. The steps described in the previous three sentences were repeated twice. Following this, a final 1mL aliquot of methanoic acid was added to the tube. Samples were stored at -20°C. Previous literature states that samples can be stored at 4°C for up to 1 year (Howe et al., 2014).

FISH Protocol for XRP XCyting Rat Chromosome Paints

To prepare a slide, the cell suspension was dropped 1cm above a Superfrost Plus slide in an environment with no less than 45% humidity (Deng et al., 2003). The ambient humidity of the

lab was tracked with a hygrometer. If ambient humidity was less than 45%, the slide was placed on a damp paper towel before the cell suspension was dropped. After the cell suspension was added, the slides were air-dried.

Once the slide was dry, 1 μ L of the XRP X Orange (X Chromosome paint, Cat# D-1521-050-OR, MetaSystems Group Inc., Medford, MA) or Y Green (Y Chromosome paint, Cat# D-1522-050-FI, MetaSystems Group Inc., Medford, MA) XCyting Rat Chromosome Paint was applied to the slide and sealed with a coverslip and rubber cement. The slide was placed on a heating plate at 75°C for 2 minutes to denature the probe. Afterward, the slide was incubated in a plastic container with a damp paper towel and distilled water at 37°C overnight for hybridization. Inside the container, the slide was set on a cell culture dish on top of the paper towel to prevent the slide from directly touching the water.

The next day, the rubber cement was gently and completely removed from the slide and the cover slide was discarded.

FISH Protocol for BAC Probes

This procedure was adapted from “DNA FISH on metaphase spreads” (Loda, 2024, kindly provided by Agnese Loda from Edith Heard’s lab at European Molecular Biology Laboratory, Heidelberg, Germany). The fluorescent *Sry*-BAC probe was prepared by Xuqi Chen using the Invitrogen FISH TagTM DNA Kit (Cat# F32947) and the rat BAC clone RNECO-180E22 encoding *Sry* 4a, 1, and 3b, the same BAC clone used to make the *Sry* transgene. The BAC clone was provided by Dr. Helen Skaletsky of MIT.

To prepare one slide, the following quantities were combined in a 1.5 mL tube and centrifuged at maximum speed for 45 minutes at 4°C: 5 μ L labeled BAC probe, 2 μ L of Salmon

Sperm ssDNA-10mg/mL, 0.7 μ L 3M sodium acetate, and 65 μ L 100% ethanol. After centrifugation, the supernatant was poured off. 500 μ L cold 70% ethanol was added for washing and the probe was centrifuged at maximum speed for 5 minutes in 4°C. The supernatant was again poured off and the probe was left open in the dark fume hood until full dry, after which 7 μ L formamide (concentration) was added. The probe was incubated at 37°C for 2 hours in a thermomixer (brand) with agitation. Next, the probes were resuspended and incubated at 75°C for 10 minutes, followed by further incubation at 37°C for 30 minutes. 100 μ L 2X hybridization buffer was prepared by combining 40 μ L of dextran sulfate diluted in water, 20 μ L of bovine serum albumin (BSA), 20 μ L 20X sodium citrate (SSC), and 10 μ L of water. This solution was vortexed gently until fully dissolved.

Cell suspension was applied to a slide as previously described for the XRP XCyting Rat Chromosome Paints, then incubated at 37°C for 24 hours. After 24 hours, the slides were washed for 10 minutes in 2X SSC (pH = 7.5) at 55°C and washed again for 5 minutes in 2X SSC (pH = 7.5) at ambient temperature (22-23°C). The slides were then dehydrated twice in 70% ethanol, once in 90% ethanol, and twice again in 100% ethanol for 5 minutes each. Once slides were dehydrated, 7 μ L of the fluorescent-labeled BAC probe was applied to the slide, followed by 7 μ L of 2X hybridization buffer. Slides were sealed with a coverslip and rubber cement, then set on a 75°C heating plate for 3 minutes to denature. Following denaturation, slides were placed in a plastic container containing a paper towel saturated with 50% formamide/2X SSC buffer. Inside the container, the slide was on a cell culture dish atop the paper towel to prevent the slide from directly touching the solution. The slides hybridized overnight.

The next day, the coverslips were removed, and the slides were washed in 2X SSC buffer for 10 minutes. They were washed two times with 0.1X SSC buffer at 55°C for 10 minutes each,

followed by one wash in 0.1X SSC buffer at room temperature for 10 minutes. The slides were set in the dark fume hood to dry. Once fully dried, the slides were stained with DAPI and sealed with a coverslip. The coverslips were sealed with a thin layer of clear nail polish around the edges. Images were taken using a Leica compound microscope.

Measuring the relative location of the transgene signal

Samples from each founder line were hybridized to the commercial Y Paint and the BAC probe as described above. Images were loaded into Adobe Photoshop. The length of the chromosome showing the transgene signal was measured in pixels. The distance between the beginning of the centromere and the location where the transgene signal begins was measured in pixels.

Statistical Analysis

Groups were compared using a Welch Two Sample t-test. Analysis was performed with R and R Studio.

RESULTS

Estrous cycle analysis shows no difference in cycle length between XX and XXY^Δ gonadal females

Vaginal swabs were taken for 21 consecutive days to observe multiple estrous cycles from each rat used in this experiment. Swabs were collected between 10 and 11 am each day to reduce variability (Cora, 2015). Vaginal cytology was classified based on the stages described in Cora et al.: proestrus (Fig. 3A), estrus (Fig. 3B), metestrus (Fig. 3C), and diestrus (Fig. 3D)

(2015). Proestrus is characterized by high levels of small nucleated epithelial cells and low levels of neutrophils, large nucleated epithelial cells, and anucleated keratinized epithelial cells. Estrus consists of high levels of anucleated epithelial cells, moderate levels of both small and large nucleated epithelial cells, and low levels of neutrophils. In metestrus, high levels of neutrophils and anucleated epithelial cells are present, as well as moderate levels of small and large nucleated epithelial cells. Lastly, diestrus contains high levels of neutrophils, moderate levels of small and large nucleated epithelial cells, and low levels of anucleated epithelial cells. As mentioned in the materials and methods section, one estrous cycle was calculated as the number in whole days between proestrus stages.

There did not appear to be a difference in estrous cycle length between XX and XXY^Δ females (Table 1) ($p=0.75$, Welch two-sample t-test). Additionally, there did not appear by eye to be any difference in cell composition for each estrous cycle stage between experimental groups.

The amount of fixative added to the final cell suspension, ambient temperature, and ambient humidity most greatly affect the spreading of chromosomes in metaphase preparations

To maximize the amount of metaphase spreads per slide, the following conditions were manipulated: volume of hypotonic solution added during fixing, amount of fixative added in the final cell suspension, angle the slide is held when the cell suspension is dropped, ambient humidity when the cell suspension is dropped, and temperature of the slide when the cell suspension is dropped. Altering the volume of added hypotonic solution influences the amount of cell swelling, so increasing the concentration of hypotonic solution consequently increases the size of the cells (Okomoda et al., 2018). In addition, decreasing the amount of fixative added to the final fixed sample increases the ratio of cells to fixative solution, and thereby raises the

quantity of cells per drop of cell suspension. Previous literature suggests holding the slide at a 45° angle when the cell suspension is dropped to encourage proper dispersion of the cell suspension onto the slide (Howe et al., 2014). Lastly, previous literature found that both ambient temperature and relative humidity affect the spreading of chromosomes within each metaphase spread (Spurbeck et al., 1996) (Deng et al., 2002). Specifically, high temperatures cause the fixative to dry too quickly, the chromosomes may not spread sufficiently (Deng et al., 2002). By this logic, low temperatures should slow the drying time, allowing the chromosomes to spread more.

With this information in mind, I hypothesized that adjusting these variables in the metaphase FISH protocol described previously would alter the number of cells producing metaphase spreads with non-overlapping chromosomes. Decreasing the amount of fixative added to the final cell suspension and increasing ambient humidity above 55% when the ambient temperature is between 20-23°C led to increases in the number of metaphase spreads achieved per slide (Table 2). Placing the slides in 4°C water for 30 minutes prior to dropping cell suspension did not appear to increase the amount of sufficiently spread chromosomes. The proportion of non-overlapping chromosomes also appeared unaffected by changing the volume of hypotonic solution added or holding the slide at a 45° angle.

Y Paint Optimization

In addition to maximizing the number of sufficiently spread metaphase chromosomes per slide, more optimization experiments were performed on the XRP XCyting Rat Chromosome Paints. Although the instructions for use list 75°C as the denaturation temperature and 37°C as the hybridization temperature, a MetaSystems representative explained that the specificity of the

probe can be affected by altering these temperatures (personal communication, Jeff Sanford, 2023).

First, changing denaturation temperature affects both the location of where the probe can hybridize to as well as the size of the hybridizing region. Sumner et al. (1971) have proposed that repetitive DNA along the chromosome is not denatured as easily as nonrepetitive DNA. Since the Y Chromosome consists mainly of heterochromatic, repetitive DNA, we hypothesized that increasing denaturation temperature might increase the amount of signal produced by Y Chromosome DNA. Alternatively, decreasing the denaturation temperature might decrease signal intensity but increase signal specificity.

Next, the composition of the hybridization buffer and the temperature of hybridization determine the probe's ability to bind to the target sequence. Since the commercial Y Chromosome paint already contains a hybridization buffer, these experiments only manipulated temperature. High hybridization temperatures increase specificity because the more energy there is in the form of heat, the more hydrogen bonds are broken between the strands of sample DNA and probe DNA (Tang et al., 2005). The more complementary base pairs that exist between a given sequence and the probe, the more hydrogen bonds exist between the two. Ideally, the temperature should be high enough to dissociate the hydrogen bonds between non-specific binding regions, or loci where the probe and sequences share a low amount of hydrogen bonds. However, it should not be too high that it dissociates all bonds between the probe and the sample DNA (Markegard et al., 2016). As a result, the temperature must be optimized to preserve hybridization between the probe and regions of high specificity, or areas where the probe and sequences share a high quantity of hydrogen bonds.

The goal of the following experiments was to determine the effect of denaturation and hybridization temperatures on probe function. Samples were collected from XXTG gonadal males from the 208 line since it is known that XXTG produces 9 signals in one metaphase spread. Slides were denatured at either 65°C, 68°C, 72°C, 75°C, 77°C, or 79°C, then hybridized overnight at either 37°C or 39°C. Overall, the probe signal produced a clear and accurate signal best at 75°C denaturation and 37°C hybridization (Fig. 5).

Discovering where Y paint hybridizes in the 208, 424, and 733 lines

Since the *Sry* BAC transgene is a Y Chromosome region, the XRP Y Green XCyting Rat Chromosome Paints was hybridized to metaphase XXTG males to determine whether it could detect the inserted portion of the Y Chromosome. Although the probe hybridizes to the Y Chromosome per its name, the safety data sheet for this commercial probe also describes cross-hybridization to Chromosomes 3, 11, and 12. In addition, Essers et al. (1995) previously found that clones of Y Chromosome repetitive sequences hybridize near the centromeres of Chromosomes 3, 11, 12, 19, and X.

The XRP Y Green paint produced eight signals in both XXWT and XYWT rats (Fig. 6). Based on chromosome morphology and previous literature, six of these signals were believed to be produced on each pair of Chromosomes 3, 11, and 19 (Fig. 6C-D, 6G-H). In XXWT females, a signal was produced on the ends of a pair of chromosomes with morphology like the X Chromosome (Fig. 6C-D). In XYWT males, a signal was produced on the end of the single X Chromosome and on the entirety of the Y Chromosome (Fig. 6G-H). This is consistent with the findings of Essers et al. (1995) and our understanding of the Pseudoautosomal Region (PAR) of the X Chromosome (Arnold, 2023) (Fig. 7C, 8C, 9C). However, there was no signal on

Chromosome 12, which is inconsistent with the results of Essers et al. (1995) and the datasheet for the XRP Y Green Paint.

The commercial Y Chromosome paint was found to hybridize nine chromosomal locations of the XXTG genome in all three founder lines. Eight of these signals (on four pairs of chromosomes) were the same as in the XXWT females and were consistent across all founder lines. The ninth signal produced by XRP Y Green Paint varied based on the founder line. In line 208, the ninth signal was determined to come from Chromosome 11 due to the chromosome's morphology, the presence of signal on Chromosome 11 discovered by Essers et al. (1995), and long-read PacBio genome sequencing analyzed by Dr. Aron Geurts at the Medical College of Wisconsin. In line 424, the ninth signal was produced on a chromosome with similar morphology to Chromosome 19 or 20 (Fig. 7); this was confirmed as belonging to Chromosome 20 using PacBio sequencing (Fig. 8). Finally, the ninth signal in line 733 was on Chromosome 2, which was supported both by rtPCR and PacBio Sequencing (Fig. 9).

BAC probe

The purpose of creating a fluorescent DNA probe of the BAC clone RNECO-180E22 was to specifically target the *Sry* TG in each of the transgenic lines, without the background staining of other chromosomes that occurs when use the commercially available Y chromosome paint. In addition, if the location of the transgene shown by the BAC probe is the same as shown by the Y Paint, this confirms the ability of the commercial Y Chromosome Paint to accurately identify the location of the transgene insertion.

Location of the transgene using Y paint & BAC probe and consistency with PAC bio sequencing

To confirm that the signal of the transgene visualized with both the commercial Y Paint and the BAC probe are consistent with the PacBio sequencing, the location of the transgene on the chromosome was calculated as a relative measurement to the size of the chromosome. The length of the chromosome containing the transgene signal was measured in pixels. The distance to the transgene was measured in pixels from one end of the chromosome to the beginning of the transgene signal. The relative location of the transgene for the Y Paint and BAC probe was calculated as a percentage by dividing the distance of the centromere to the transgene by the total length of the chromosome containing the transgene.

In the 208 line, the average location of the transgene was $60.41\% \pm 4.69\%$ for the Y Paint (n=19, median = 59.64%) (Table 4) and $59.75\% \pm 4.37\%$ for the BAC probe (n=12, median = 59.99%) (Table 45). In the 424 line, the average location of the transgene was $51.26\% \pm 4.18\%$ for the Y Paint (n=3, median = 52.89%) (Table 6) and $44.79\% \pm 7.54\%$ for the BAC probe (n=11, median = 43.43%) (Table 7). In the 733 line, the average location of the transgene was $32.02\% \pm 4.99\%$ for the Y Paint (n=13, median = 31.30%) (Table 8) and $31.51\% \pm 4.49\%$ for the BAC probe (n=4, median = 31.68%) (Table 9).

X Paint Hybridization Location

Since the XRP Y Green XCyting Rat Chromosome Paint hybridized to parts of the genome besides the Y Chromosome, we decided to test the XRP X Orange XCyting Rat Chromosome Paint as well for additional binding sites. The commercial X Chromosome paint appears to only hybridize with the X Chromosome and produces 1 signal in XYWT animals and 2 signals in XXWT animals (Fig. 6).

Confirming genotyping of XYY^Δ gonadal males with the BAC probe

The BAC probe was applied to fixed metaphase spreads of XYY^Δ males to confirm PCR genotyping. Hybridization to the BAC probe should theoretically hybridize to both the Y and Y^Δ Chromosomes. Following this theory, there appears to be a signal on both chromosomes with morphology like the Y Chromosome (Fig. 14).

DISCUSSION

The overall goal of this series of experiments was to determine important hormonal and genetic characteristics of our new Sry-modified rat models, a means of quality assurance.

First, the goal of measuring estrous cycles in XX females and XXY^Δ females was to determine whether these genotypes show differences in hypothalamic-pituitary-gonadal function that would be revealed by the timing of the estrous cycle. If the HPG function is the same between XX and XXY^Δ gonadal females, then we have evidence that any phenotypic differences between these groups may not be caused by a difference in HPG function. No differences in estrous cycle length or vaginal cytology analysis were observed (Fig. 2) (Table 1), implying the absence of any differences in hormone concentrations between the gonadal females that would affect estrous cycle length. Of course, other measurements could reveal hormonal differences that would not affect estrous cycle length.

Next, localizing the transgene is important for determining if it may have positional effects. If the transgene is inserted within a gene or regulatory region, it can interfere with that gene's expression, which could confound the results of experiments interested in that gene. Although FISH does not allow us to determine the location of the gene in base pairs, locating the

chromosomal position of the transgene provide useful confirmation of our PCR and PacBio long-read DNA sequencing data.

Since the insertion site of the transgene during CRISPR is random, we expected to find the *Sry* transgenes at different locations in each of our founder lines (Banakar et al., 2019). Before any experiments to find the transgene were conducted, however, a series of protocol optimization experiments were conducted to improve cost-effectiveness.

The first of these manipulated conditions of the metaphase slide preparation process. Increasing the number of clear, non-overlapping spreads of metaphase chromosomes obtained per slide would increase the data collected and reduce the materials cost during experiments. Overall, the most effective methods of increasing metaphase spread count were decreasing the amount of methanoic-acetic fixative added to the final cell suspension and increasing the ambient humidity to no less than 55%. It makes sense that decreasing the amount of fixative added increases the number of metaphase spreads per slide because this increases the number of fixed cells in each drop of cell suspension. In addition, increasing the ambient humidity when the cell suspension is dropped increases the amount of metaphase spreads because of the added process of dynamic rehydration. When methanoic acid fixative absorbs water from the air, it releases a large amount of free energy (Deng et al., 2003). This phenomenon is termed dynamic rehydration, and the energy released in this process is theorized to increase the amount of energy for chromosome spreading and push them further apart from one another.

In addition to metaphase spread count, more experiments were carried out to find the optimal denaturation temperatures of Metasystems Y Chromosome paint. As mentioned in the results, the temperature at which the probe is denatured onto the slide is critical for separating the DNA into single strands accessible to the probe. However, the optimal denaturation temperature

depends on the composition of the target sequence. Specifically, the base pairs cytosine (C) and guanine (G) share three bonds, whereas adenine (A) and thymine (T) only share two. Since it takes more energy (in the form of heat) to break the bonds between Cs and Gs, denaturation temperatures must be higher for target sequences containing more pyrimidines. *Sry* specifically comes from the Y Chromosome, which primarily consists of heterochromatin (Charlesworth, 2003). Compared to its counterpart, euchromatin, heterochromatin is gene-poor and has a higher CG% [cite]. For this reason, we hypothesized that increasing the temperature would increase the amount of signal produced by Y Chromosome DNA while decreasing the denaturation temperature would decrease signal intensity but increase signal specificity. We tested conditions both higher and lower than the recommended denaturation temperature of 75°C. In the end, we found that 75° produced the strongest signal. Furthermore, temperatures above 75° and below 68° resulted in little to no signal present.

The first approach taken to find the *Sry* transgene was using a commercially available Y Chromosome paint on XX gonadal males. While these animals do not possess an entire Y Chromosome, we hypothesized that the Y Chromosome paint could detect the transgene because *Sry* is a Y Chromosome gene. The XRP Y Green Paint produced a signal at nine locations in each of the founder lines. Eight of these hybridization sites were the same across all founder lines: on both sets of Chromosomes 3, 11, 19, and X.

The finding that there are repetitive sequences between the Y Chromosome and Chromosomes 3, 11, and 19 was first documented by Essers et. al (1995) using hybridization of clones of Y DNA allowed to reassociate after DNA shearing. As for the X Chromosome signal, the appearance of the signal at the end of the chromosome might represent the Pseudoautosomal Region (PAR) of the X Chromosome, or the centromere. The PAR is a region of shared genes

between the X and Y Chromosome and is the only location where these chromosomes presumably recombine (Arnold, 2023). The similarity of XPAR and YPAR could account for the binding of the Y paint to the X chromosomes. However, this cannot be confirmed because the PAR of the Sprague-Dawley rat genome is not yet sequenced.

One inconsistency between the literature and the current findings is the apparent lack of signal on Chromosome 12. The safety data sheet for the XRP Y Green Paint states that signal was also seen on the short arms of rat Chromosome 12; Essers et al. (1995) also found common repetitive sequences between Chromosomes 12 and Y. However, no signal was produced on Chromosome 12 when the XRP Y Green Paint was applied (Figs. 6-9). Although further experimentation is needed to confirm why this occurs, possible explanations for this could be the sequence of the commercial Y Paint, the size of the repetitive region on Chromosome 12, or a low level of specificity between this region and the probe.

Unlike the previous eight, the ninth signal produced by the Y Chromosome was different in XXTG cells from transgenic lines 208, 424, and 733. The location of this signal was Chromosome 11 in the 208 line (Fig. 7), Chromosome 20 in the 424 line (Fig. 8), and Chromosome 2 in the 733 line (Fig. 9). Since we already knew from genome sequencing that the transgene in the line 733 was inserted into Chromosome 2, this improved the credibility of the results seen from the 424 and 733 lines. Thus, it appears that DNA FISH using the XRP Y Green Chromosome Paint is an effective means of visualizing the insertion site of the *Sry* BAC transgene.

The second means of visualizing the *Sry* transgene was through a fluorescent BAC probe containing the same sequence as the transgene. The reason for this is twofold: first, this probe contains the same sequence as the transgene, making it a more specific hybridization probe than

the commercial Y Chromosome paint. Second, if the location of the transgene detected by the BAC probe is the same as the ninth signal produced by the Y Paint, the Y Paint can be confirmed as a legitimate method for finding some Y Chromosome transgenes in genetically modified organisms. The BAC probe was made using a Nick translation protocol and the hybridization process was carried out in accordance with the protocol from the Heard Lab. From this experiment, we found that the BAC probe produces signal on Chromosome 11 of the 208 founder line, Chromosome 20 of the 424 line, and Chromosome 2 of the 733 line. This finding is consistent with the results of the Y Paint experiments, as well as PacBio Sequencing performed by our collaborator Dr. Geurts.

To determine if the transgene signal was produced at a consistent location in each of the founder lines, the location of the transgene relative to the length of the chromosome it was found in was measured as a percentage of the distance from the centromere of the chromosome. Overall, the location of the transgene was consistent among samples from the same line, in each of the lines.

Lastly, since the commercial Y Chromosome paint was found to have hybridization locations outside of the Y Chromosome, we used a commercial X Chromosome paint to identify whether X Chromosome sequences were present in regions of the rat genome besides the X Chromosome. These experiments were performed using the same protocol for the Y Chromosome paint. The only signal produced was belonging to the X Chromosome(s); this was consistent regardless of the number of X Chromosomes present in each sample. For instance, only one signal was produced when applied to XYWT animals and 2 when applied to XXWT. This implies that sequences detected by the X Chromosome paint are exclusive to the X

Chromosome. Additionally, it suggests that the sequence of the X Chromosome is unlike that of any other chromosome.

CONCLUSION

This research sought to compare estrous cycle length in XX and XXY^Δ gonadal females and find the location of the *Sry* transgene insertion site in transgenic animals of each of the founder lines. Quantitative analysis of the estrous cycles of XX and XXY^Δ females revealed no significant difference in cycle length, and therefore did not reveal any difference in HPG function. In addition, both the Metasystems XRP Y Green XCyting Rat Chromosome Paint and the RNECO-180E22 BAC probe showed the location of the transgene was consistent among samples from the same line, in each of the lines.

FIGURES

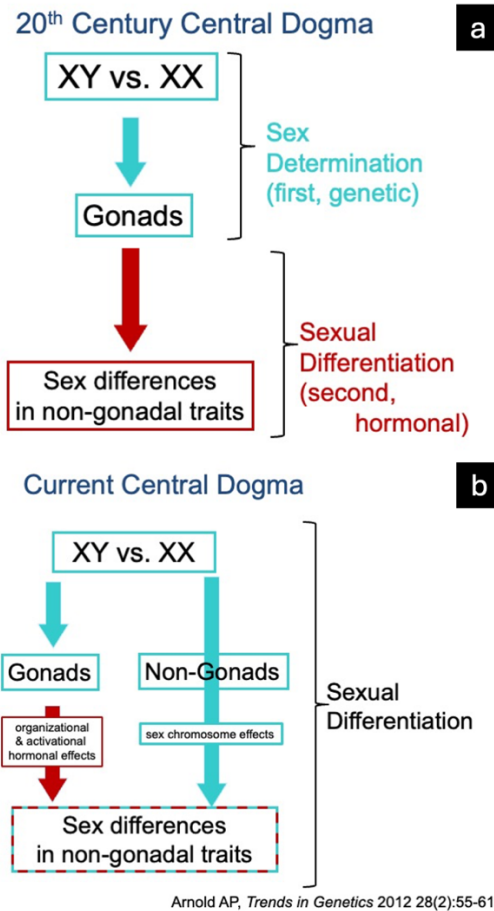


Figure 1: Overview of differences in dogma between the 20th and 21st centuries. This graphical overview illustrates the ideological shift in sexual differentiation theory between the 20th century and now. (a) In the 20th century, the sex chromosomes were thought to determine the gonads, and the hormones released from the gonads were what caused other phenotypic sex differences. (b) While the sex chromosomes are still believed to determine the gonads, it is now recognized that sex chromosome genes can directly influence phenotypic sex differences as well.

Note: Based on “The organizational-activational hypothesis as the foundation for a unified theory of sexual differentiation of all mammalian tissues,” by Arthur P. Arnold (2009).

Hormones and behavior, 55(5), 570-578.

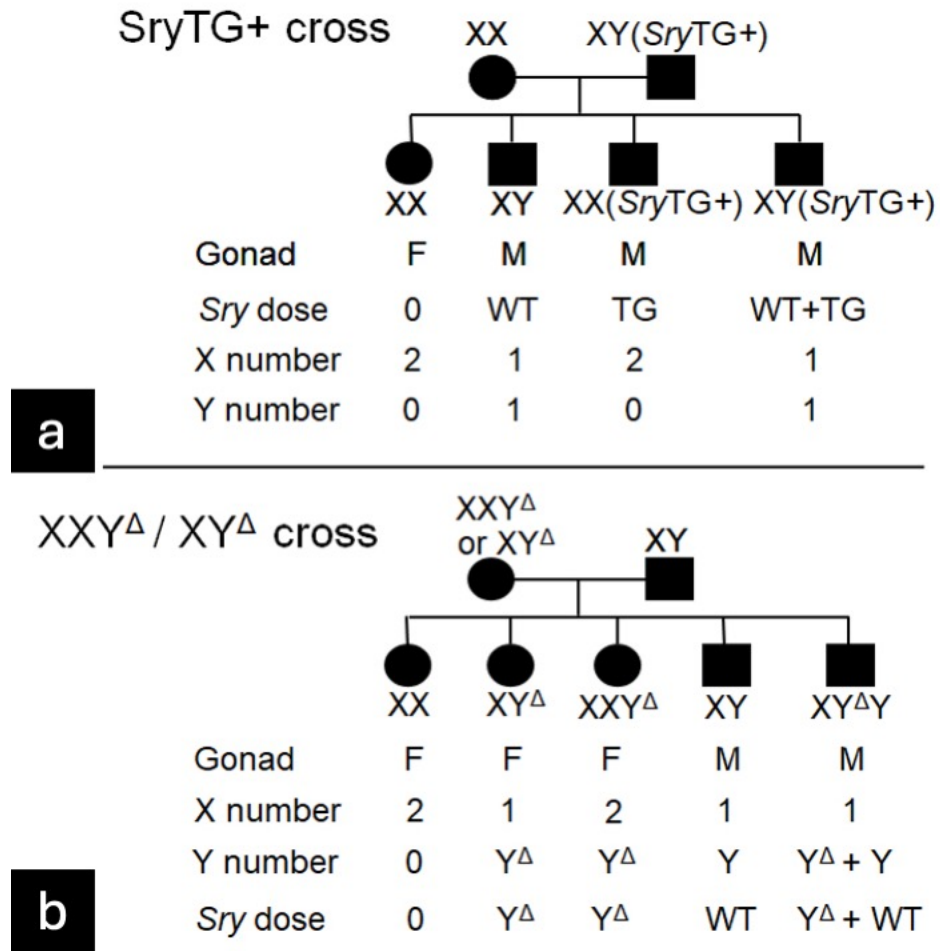


Figure 2: Breeding Scheme of rats in the *Tdf*-KO model. Two crosses required to produce the *Sry*-manipulated rat model. (a) Breeding an XX wild-type female with an XY(*Sry*TG+) animal produces wild-type gonadal females (XXF), wild-type gonadal males (XYM), XX transgenic males (XXM) and XY males with the *Sry* transgene (XYM(*Sry*TG+)) (Arnold et al., 2023). (b) Breeding an XY^Δ or XXY^Δ female with a wild-type XY male produces wild-type gonadal females (XXF), wild-type gonadal males (XYM), XY^Δ females (XYF), XXY^Δ females (XXYF), and XYY^Δ males (XYYM). Breeding of XXY^Δ females does not produce XY^Δ daughters.

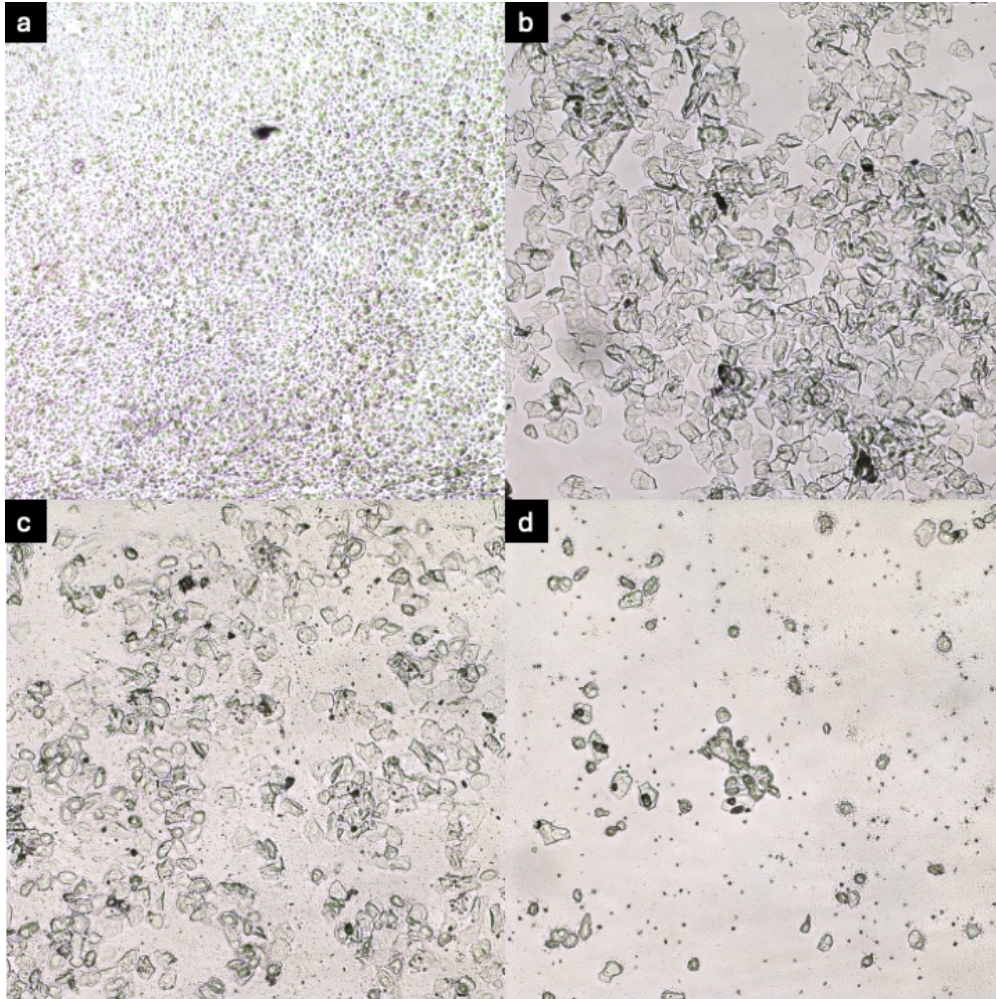


Figure 3: Vaginal cytology of each estrous cycle stage. Vaginal smears were collected at between 10 and 11 AM each day for 24 days. The tips of cotton swabs were dipped in 1X PBS before smears, and the smears were mounted on slides. (a) Proestrus has high levels of small nucleated epithelial cells and low levels of neutrophils, large nucleated epithelial cells, and anucleated keratinized epithelial cells. (b) Estrus has high levels of anucleated epithelial cells, moderate levels of small and large nucleated epithelial cells, and low levels of neutrophils. (c) Metestrus has high levels of neutrophils and anucleated epithelial cells, and moderate levels of small and large nucleated epithelial cells. (d) Diestrus has high levels of neutrophils, moderate levels of small and large nucleated epithelial cells, and low levels of anucleated epithelial cells.

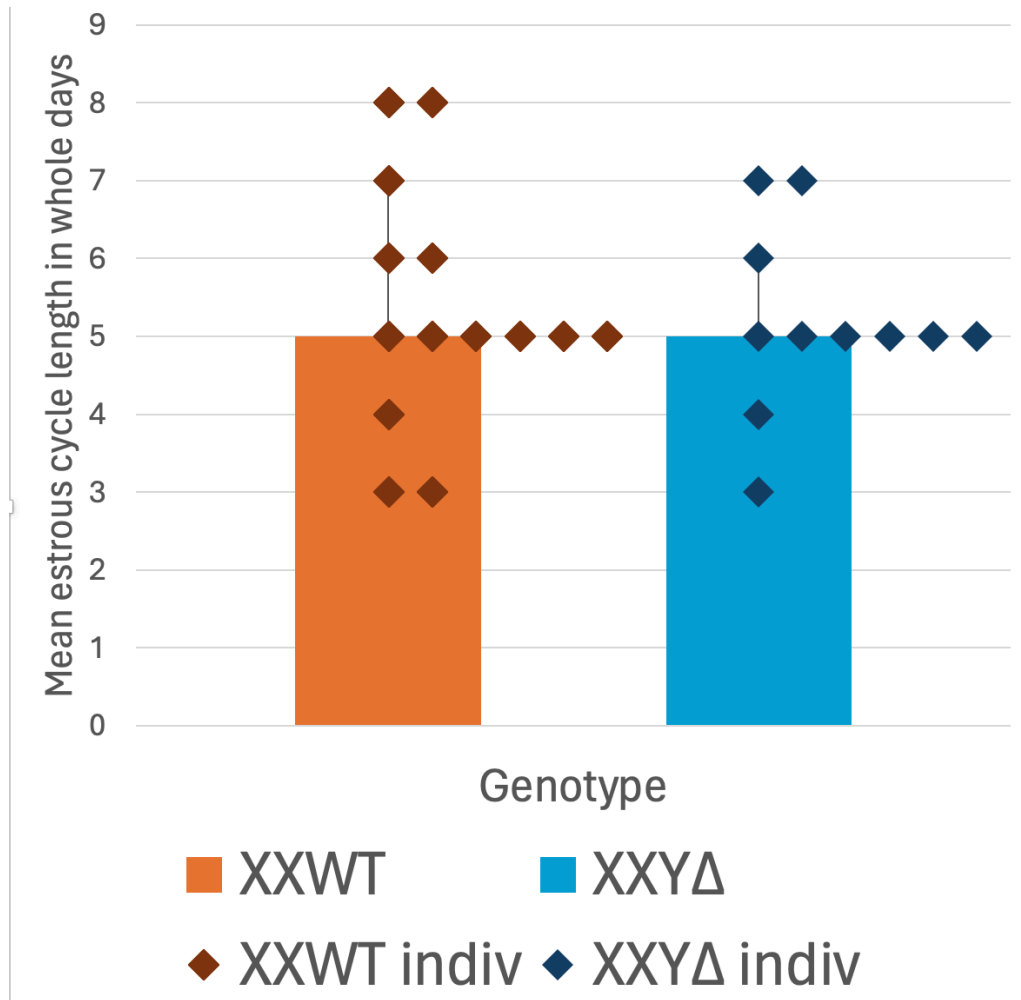


Figure 4: Comparison of mean estrous cycle length in whole days between XX and XXY^Δ gonadal females. Methods used to collect samples are described in Fig. 3. One estrous cycle was calculated as the number in whole days between proestrus stages. A Welch's Two Sample T-Test was used to compare the mean estrous cycle length of each rat across both groups.

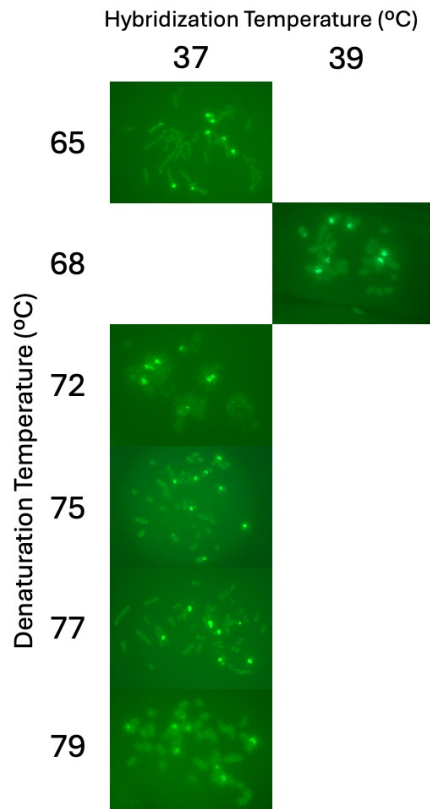


Figure 5: Optimization of denaturation and hybridization temperatures for the Metasystems XRP Y Green XCyting Rat Chromosome Paint. Samples were collected from XXTG gonadal males from the 208 line. Metaphase spreads were prepared by growing and harvesting rat tail tip fibroblast cells and fixing them in 3:1 methanoic acid, and applying the Metasystems Green XCyting Rat Chromosome Paint (XRP Y Green) (Order #D-1522-050-FI). Slides were denatured at either 65°C, 68°C, 72°C, 75°C, 77°C, or 79°C, then hybridized overnight at either 37°C or 39°C. Denaturation at 75°C and hybridization at 37°C produced the most consistent and clear results. Denaturation temperatures of 72°C or below and 79°C or higher resulted in chromosome labeling that looked fuzzy and did not always produce the expected nine signals typically seen when the XRP Y Green Paint is applied to XXTG gonadal males. This unclear labelling was also seen in the 39°C hybridization group.

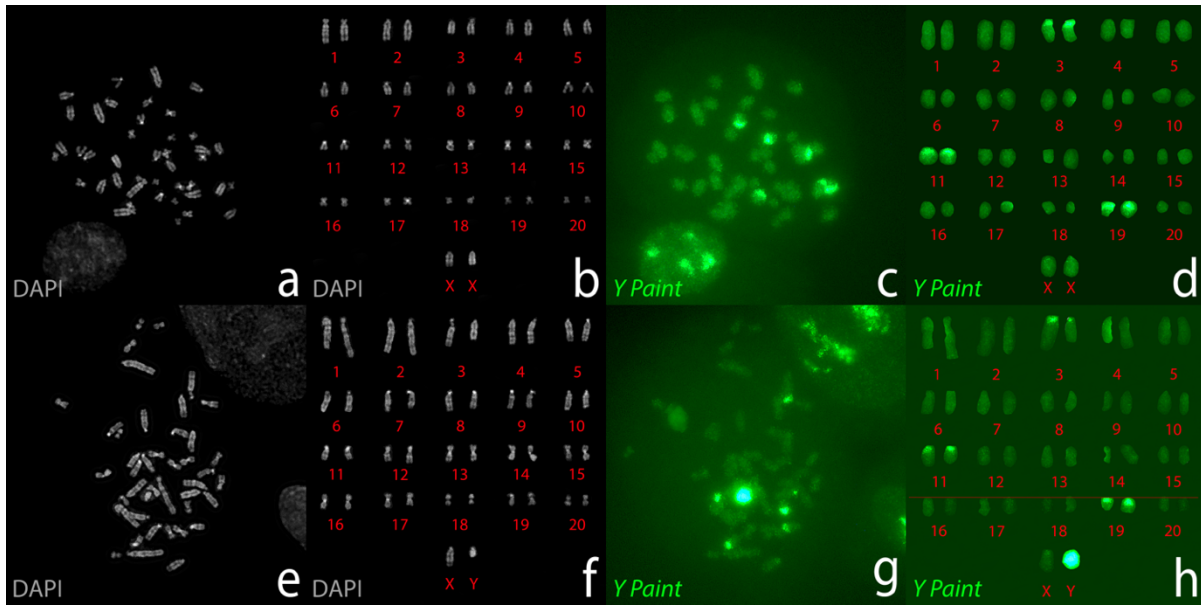


Figure 6: Using the commercial Y Chromosome Paint on an XXWT female and XYWT male..

The XRP Y Green Paint was denatured on the slide at 75°C and hybridized overnight at 37°C. After hybridization, DAPI/Antifade (D-0902-500-DA) was applied. Chromosomes were imaged using a Leica DM1000 LED Ergonomic system microscope and sorted by morphology per the *Rattus norvegicus* ideograms presented by Hamta et al., 2006. (a) Metaphase chromosomes from an XXWT rat labeled by DAPI. (b) The DAPI stained chromosomes in karyotype analysis. (c) Metaphase chromosomes from an XXWT rat labeled with XRP Y Green. (d) The XRP Y Green in karyotype analysis. (e) Metaphase chromosomes from an XYWT rat labeled by DAPI. (f) The DAPI stained chromosomes in karyotype analysis. (g) Metaphase chromosomes from an XYWT rat labeled with XRP Y Green. (h) The XRP Y Green in karyotype analysis. XXWT rats produce 8 signals and XYWT rats produce 8 signals when hybridized the MetaSystems XRP Y Green XCyting Rat Chromosome Paint.

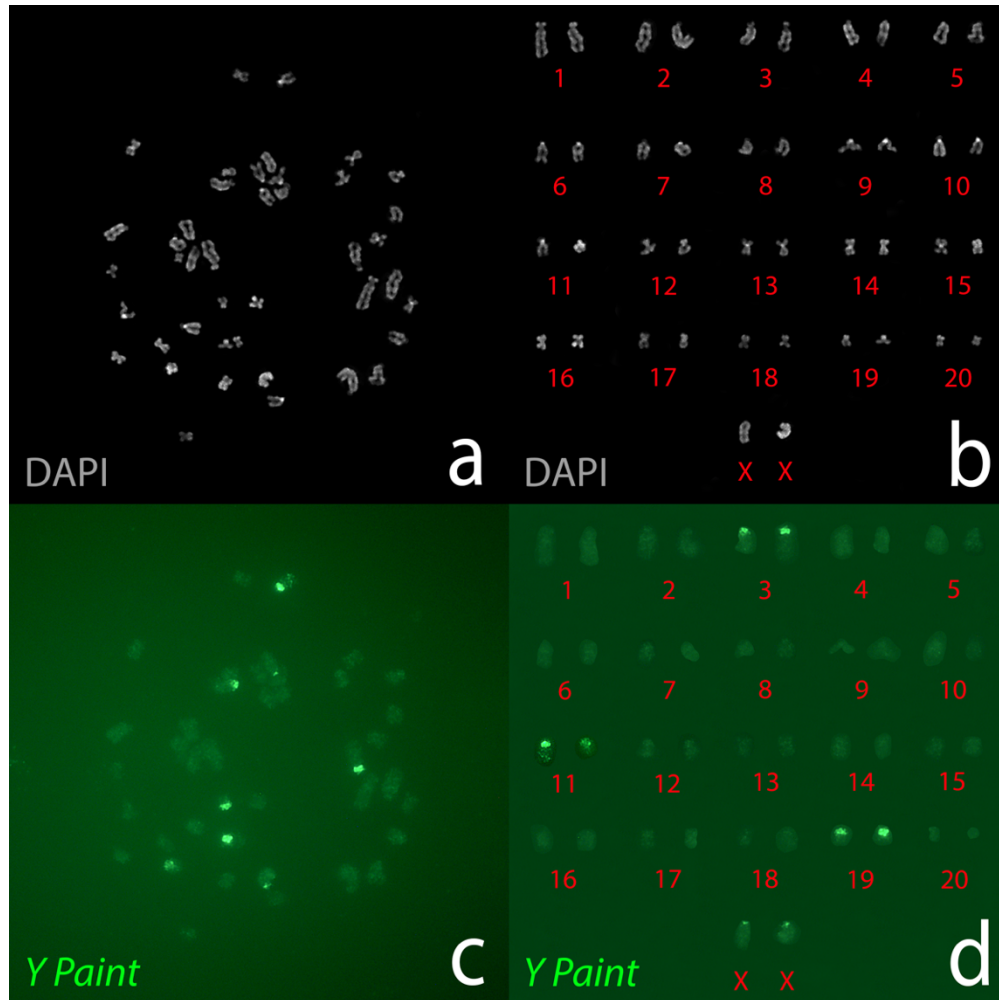


Figure 7: Using the commercial Y Chromosome Paint to locate the Sry-transgene on Chromosome 11 in 208N14:3, an XXTG male from the 208 line. Methods used are described in Fig. 6. (a) Metaphase chromosomes labeled by DAPI. (b) The DAPI stained chromosomes in karyotype analysis. (c) Metaphase chromosomes labeled with XRP Y Green. (d) The XRP Y Green labels chromosome pairs 3,11,19, and X, and a second position on one Chromosome 11 at the location of the transgene.

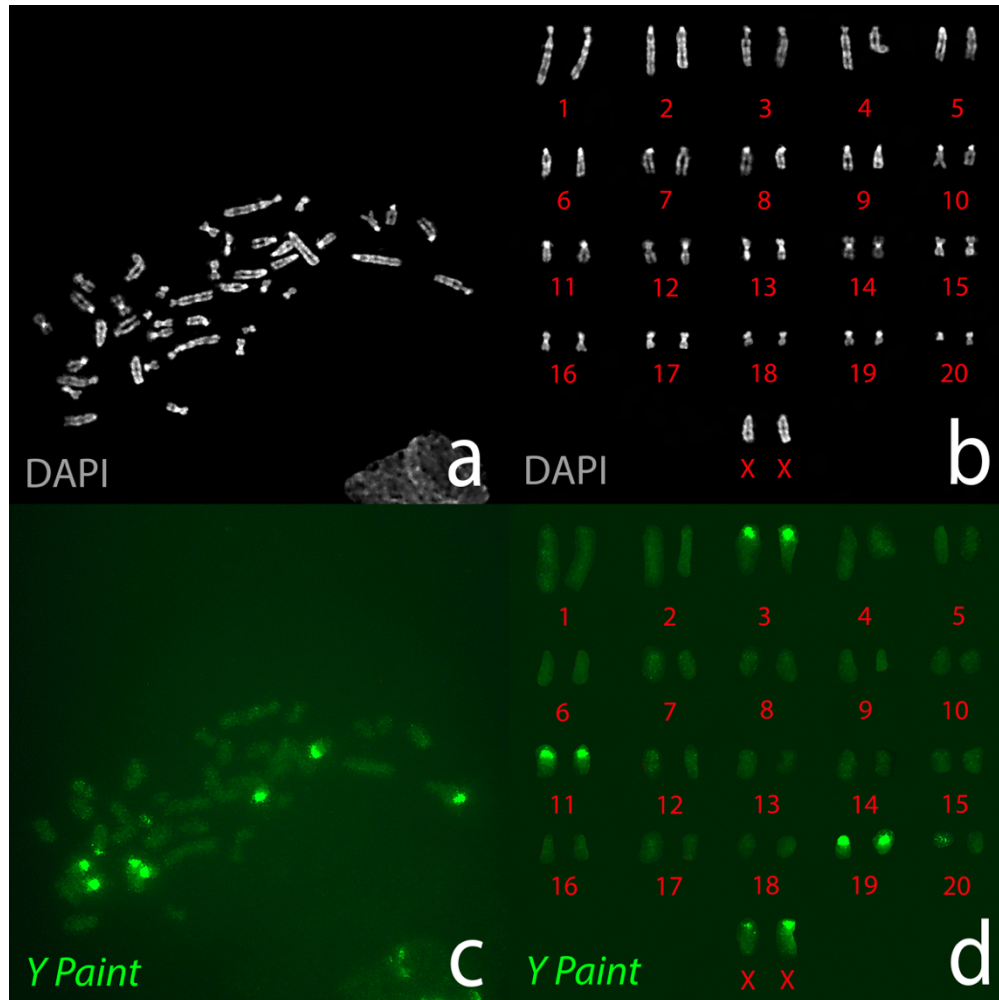


Figure 8: Using the commercial Y Chromosome Paint to locate the *Sry*-transgene on Chromosome 20 in 424N12:2:2, an XXTG male from the 424 line. Methods used are described in Fig. 6. (a) Metaphase chromosomes labeled by DAPI. (b) The DAPI stained chromosomes in karyotype analysis. (c) Metaphase chromosomes labeled with XRP Y Green. (d) The XRP Y Green in karyotype analysis. XXTG gonadal males produce 9 signals when hybridized the XRP Y Green XCyting Rat Chromosome Paint, including to the line-specific *Sry*-transgene insertion site in Chromosome 20.

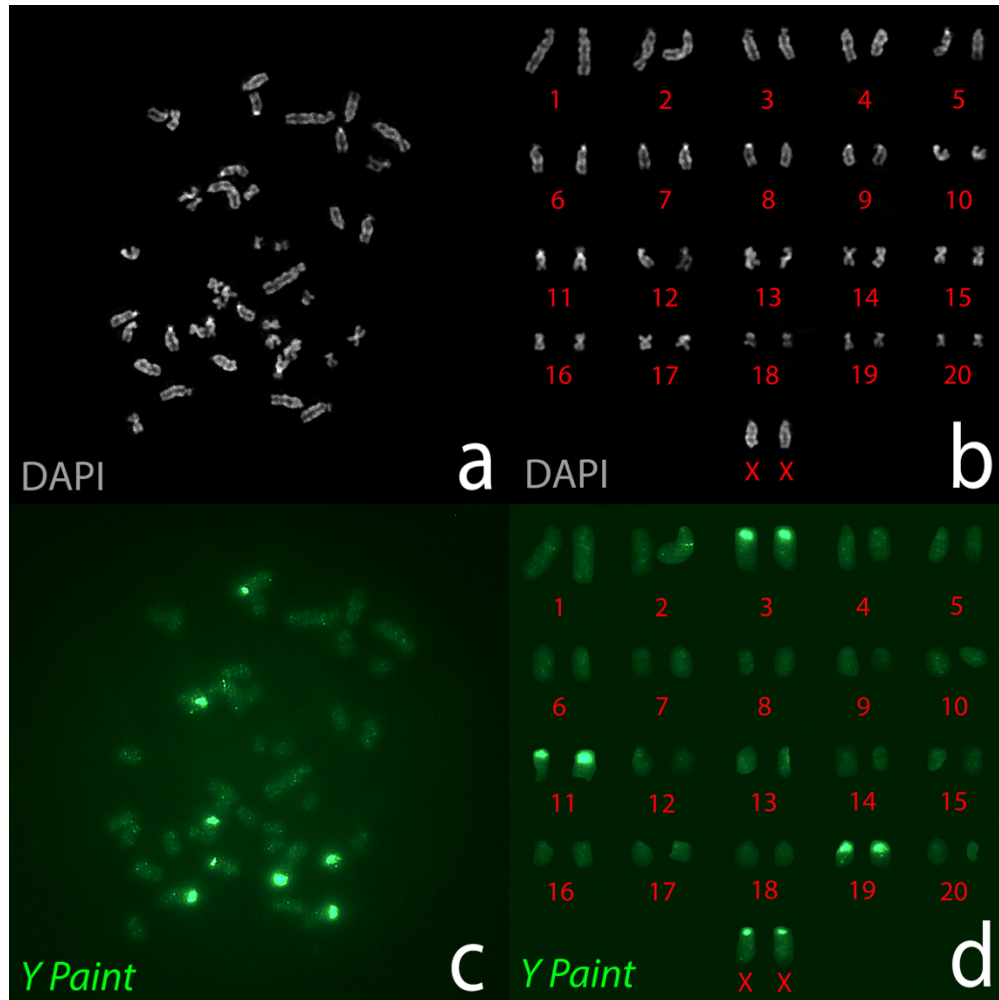


Figure 9: Using the commercial Y Chromosome Paint to locate the *Sry*-transgene on Chromosome 2 in 733N12:1, an XXTG male from the 733 line. Methods used are described in Fig. 6. (a) Metaphase chromosomes labeled by DAPI. (b) The DAPI stained chromosomes in karyotype analysis. (c) Metaphase chromosomes labeled with XRP Y Green. (d) The XRP Y Green in karyotype analysis. XXTG gonadal males produce 9 signals when hybridized the XRP Y Green XCyting Rat Chromosome Paint, including to the line-specific *Sry*-transgene insertion site in Chromosome 2.

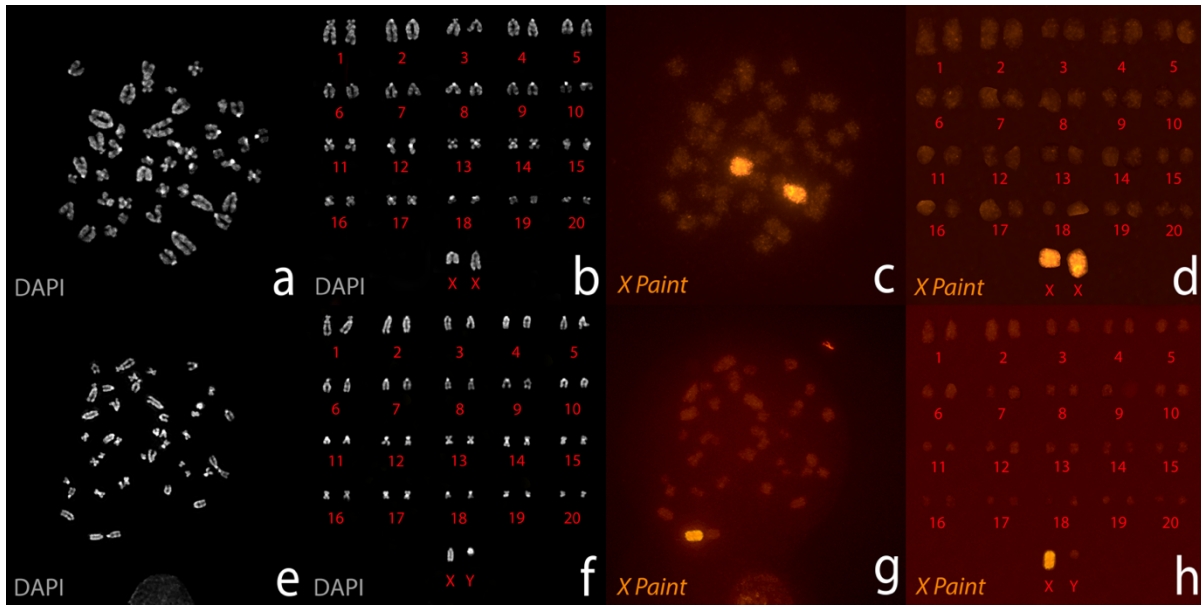


Figure 10: Using the XRP X Orange XCyting Rat Chromosome Paint on an XXWT female and XYWT male. Metaphase spreads were prepared by growing and harvesting rat tail tip fibroblast cells and fixing them in 3:1 methanoic acid. The XRP X Orange Paint was denatured on the slide at 75°C and hybridized overnight at 37°C. After hybridization, DAPI/Antifade (D-0902-500-DA) was applied. Chromosomes were imaged using a Leica DM1000 LED Ergonomic system microscope and sorted by morphology per the *Rattus norvegicus* ideograms presented by Hamta et al., 2006. (a) Metaphase chromosomes from an XXWT rat labeled by DAPI. (b) The DAPI stained chromosomes in karyotype analysis. (c) Metaphase chromosomes from an XXWT rat labeled with XRP X Orange. (d) The XRP X Orange in karyotype analysis. (e) Metaphase chromosomes from an XYWT rat labeled by DAPI. (f) The DAPI stained chromosomes in karyotype analysis. (g) Metaphase chromosomes from an XYWT rat labeled with XRP X Orange. (h) The XRP X Orange in karyotype analysis. XXWT rats produce 2 signals and XYWT rats produce 1 signal when hybridizing the MetaSystems XRP X Orange X Cyting Rat Chromosome Paint.

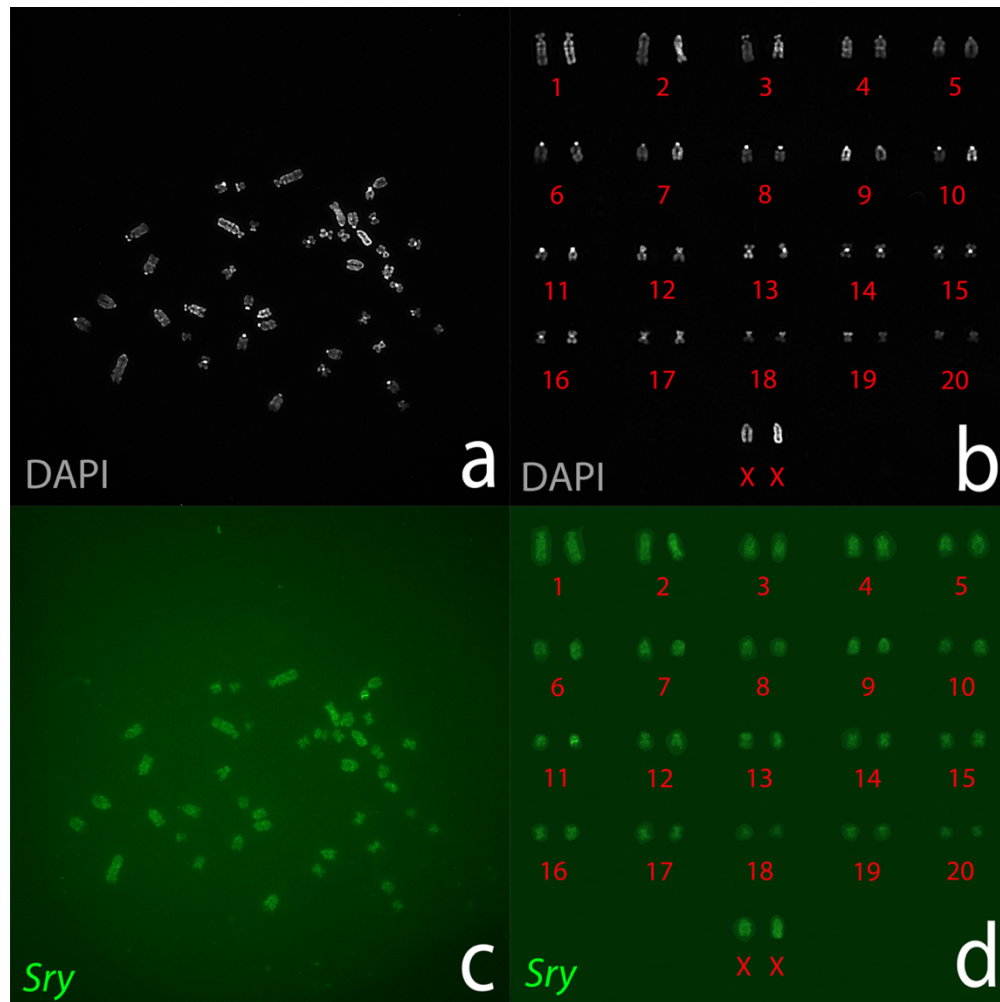


Figure 11: Using the BAC clone RNECO-180E22 probe to locate the *Sry*-transgene on Chromosome 11 in 208N14:3, an XXTG male from the 208 line. Metaphase spreads were prepared as described in Fig. 7. The BAC probe was denatured at 75°C and hybridized overnight at 37°C. After hybridization, DAPI/Antifade (D-0902-500-DA) was applied. Chromosomes were imaged using a Leica DM1000 LED Ergonomic system microscope and sorted by morphology per the *Rattus norvegicus* ideograms presented by Hamta et al., 2006. (a) Metaphase chromosomes labeled by DAPI. (b) The DAPI stained chromosomes in karyotype analysis. (c) Metaphase chromosomes labeled with the BAC probe. (d) The BAC probe in karyotype analysis. The BAC hybridizes to the line-specific *Sry*-transgene insertion site in Chromosome 11.

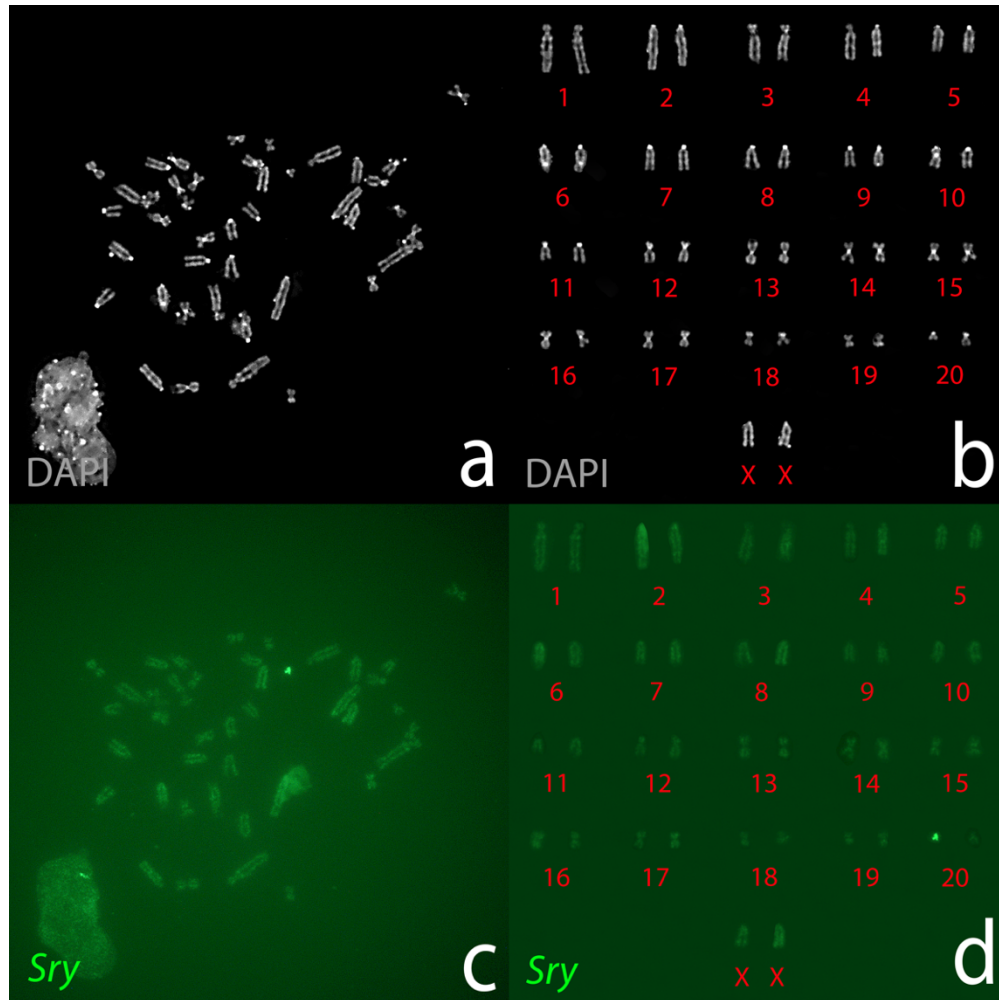


Figure 12: Using the BAC clone RNECO-180E22 probe to locate the *Sry*-transgene on Chromosome 20 in 424N12:4:1, an *XXTG* male from the 424 line. Methods used are described in Fig. 11. (a) Metaphase chromosomes labeled by DAPI. (b) The DAPI stained chromosomes in karyotype analysis. (c) Metaphase chromosomes labeled with the BAC probe. (d) The BAC probe in karyotype analysis. The BAC hybridizes to the line-specific *Sry*-transgene insertion site in Chromosome 20.

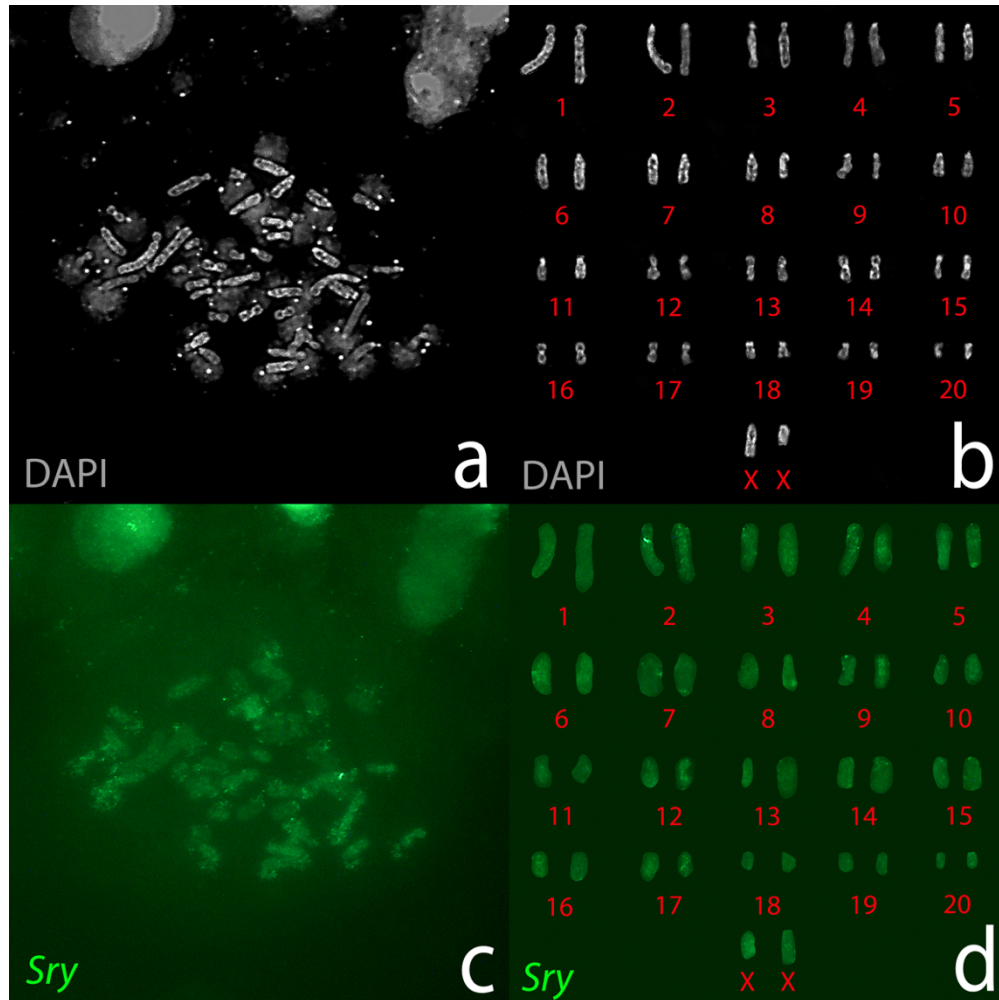


Figure 13: Using the BAC clone RNECO-180E22 probe to locate the *Sry*-transgene on Chromosome 2 in 733N12:2:5, an *XXTG* male from the 733 line. Methods used are described in Fig. 11. (a) Metaphase chromosomes labeled by DAPI. (b) The DAPI stained chromosomes in karyotype analysis. (c) Metaphase chromosomes labeled with the BAC probe. (d) The BAC probe in karyotype analysis. The BAC hybridizes to the line-specific *Sry*-transgene insertion site in Chromosome 2.

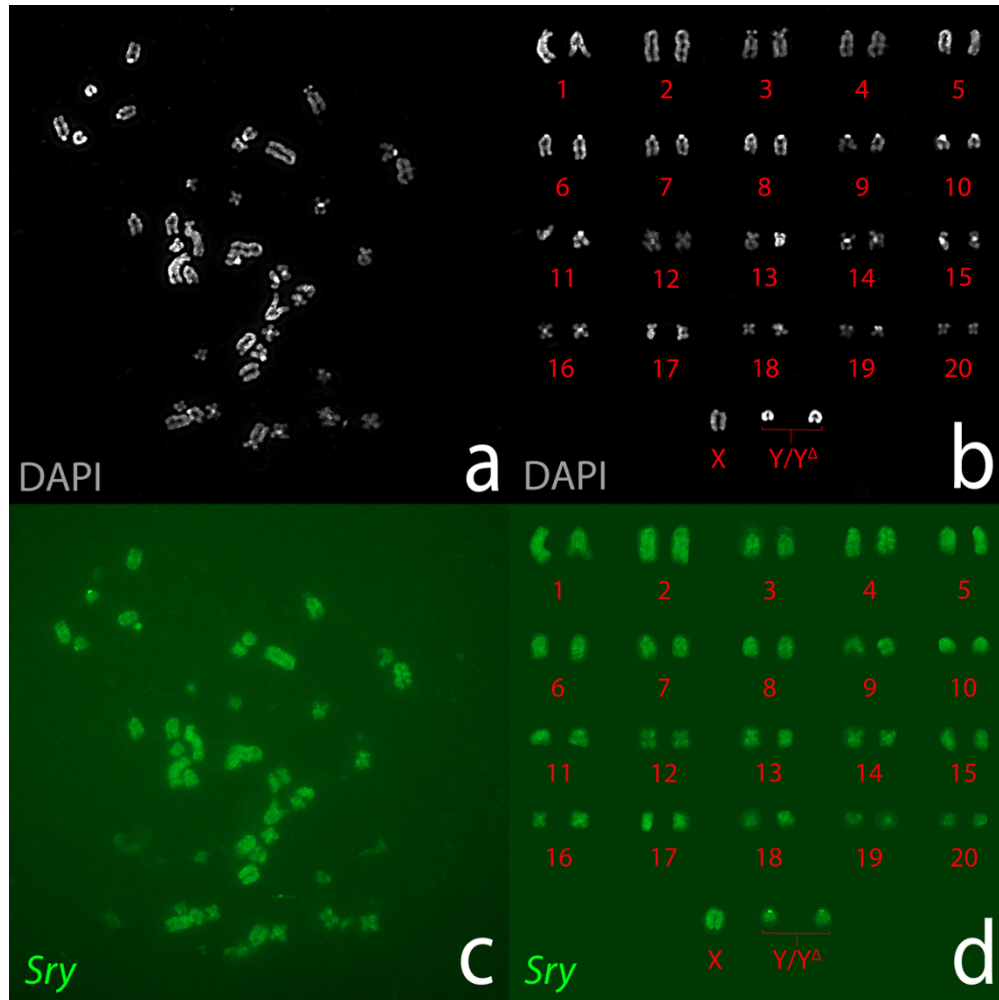


Figure 14: Using the BAC clone RNECO-180E22 probe to locate the *Sry*-transgene in *XYFrN12:4:1*, an $XY Y^\Delta$ male from the *XYFr* line. Methods used are described in Fig. 11. (a) Metaphase chromosomes labeled by DAPI. (b) The DAPI stained chromosomes in karyotype analysis. (c) Metaphase chromosomes labeled with the BAC probe. (d) The BAC probe in karyotype analysis. The BAC hybridizes to the Y and Y^Δ Chromosomes.

TABLES

Table 1: Estrous cycle data: Vaginal smears were collected at between 10 and 11 am each day for 24 days. The tips of cotton swabs were dipped in 1X PBS before smears, and the smears were mounted on slides. One whole estrous cycle was counted as One full estrous cycle was calculated as the number in whole days between proestrus stages.

<i>Mean Estrous Cycle Lengths of XXWT and XXYΔ Gonadal Females in Whole Days</i>			
<i>XXWT</i>		<i>XXYΔ</i>	
Animal ID	Mean Cycle Length (Whole Days)	Animal ID	Mean Cycle Length (Whole Days)
XYFrN9:12:6	5	XYFrN9:12:4	4
XYFrN10:4:2	4	XYFrN9:12:5	5
XYFrN10:4:6	6	XYFrN10:4:8	7
XYFrN10:5:1	7	XYFrN10:4:9	6
XYFrN10:5:2	5	XYFrN10:5:3	5
XYFrN9:15:3	5	XYFrN9:15:2	5
XYFrN9:15:5	5	XYFrN9:15:4	5
XYFrN10:13:1	5	XYFrN10:13:3	7
XYFrN10:13:4	3	XYFrN10:17:1	5
XYFrN10:18:1	8	XYFrN10:19:2	3
XYFrN10:18:2	3	XYFrN11:5	5
XYFrN10:19:1	8	Mean	5
XYFrN10:19:3	6	Standard Deviation	1
XYFrN11:4	5	Median	5
Mean	5		
Standard Deviation	2		
Median	5		

Table 2: Maximizing metaphase spreads

Metaphase Optimization Conditions								
Slide Number	Final [Fixative] (mL)	Slide Angle	Water Vapor	Cold Slide	Cell Count	Metaphase Spread Count	% metaphases /spreads	
1	0.25	0°	No	No	2300	81	3.52%	
2	0.25	0°	No	Yes	1446	59	4.08%	
3	0.25	45°	No	No	1153	45	3.90%	
4	0.25	0°	No	Yes	1558	19	1.22%	
5	0.25	0°	Yes	No	866	15	1.73%	
6	0.25	0°	No	No	1684	11	0.65%	
7	0.25	45°	No	No	918	10	1.09%	
8	0.25	45°	No	No	731	10	1.37%	
9	0.5	0°	No	No	1109	9	0.81%	
10	0.5	0°	Yes	No	263	9	3.42%	
11	0.5	0°	No	No	547	6	1.10%	
12	0.5	0°	No	Yes	834	5	0.60%	
13	0.5	0°	No	Yes	420	5	1.19%	
14	0.5	0°	No	Yes	381	5	1.31%	
15	0.5	0°	No	No	656	5	0.76%	
16	0.5	45°	No	No	463	5	1.08%	
17	0.75	0°	Yes	No	700	4	0.57%	
18	0.75	0°	Yes	No	232	4	1.72%	
19	0.75	45°	No	No	351	3	0.85%	
20	0.75	0°	Yes	No	194	2	1.03%	
21	1	45°	No	No	571	1	0.18%	
22	1	0°	Yes	No	170	1	0.59%	
23	1	0°	No	No	158	0	0.00%	
24	1	0°	No	Yes	555	0	0.00%	

Table 3: XXTG using MetaSystems XRP Y Green XCyting Rat Chromosome Paint

TG information for XRP Y Green in XCyting Rat Chromosome Paint in XXTG Gonadal Males			
<i>Founder Line</i>	<i>Mean location of Sry transgene signal as a % of the chromosome length</i>	<i>Standard deviation of mean location of Sry transgene signal as a % of the chromosome length</i>	<i>Median location of Sry transgene signal as a % of the chromosome length²</i>
208 (n=17)	60.41%	±4.69%	59.64%
424 (n=3)	51.26%	±4.18%	52.89%
733 (n=13)	32.02%	±4.99%	31.30%

Table 4: XXTG using the BAC Clone RNECO-180E22 Probe

TG information for the BAC Clone RNECO-180E22 Probe in XXTG Gonadal Males			
<i>Founder Line</i>	<i>Mean location of Sry transgene signal as a % of the chromosome length</i>	<i>Standard deviation of mean location of Sry transgene signal as a % of the chromosome length</i>	<i>Median location of Sry transgene signal as a % of the chromosome length²</i>
208 (n=12)	59.75%	4.37%	59.99%
424 (n=11)	44.79%	7.54%	43.43%
733 (n=4)	31.51%	4.49%	31.68%

REFERENCES

- Arnold, A. P. (2009). The organizational–activational hypothesis as the foundation for a unified theory of sexual differentiation of all mammalian tissues. *Hormones and Behavior*, 55(5), 570–578. <https://doi.org/10.1016/j.yhbeh.2009.03.011>
- Arnold, A. P. (2012). The end of gonad-centric sex determination in mammals. *Trends in Genetics: TIG*, 28(2), 55–61. <https://doi.org/10.1016/j.tig.2011.10.004>
- Arnold, A. P. (2017). A general theory of sexual differentiation. *Journal of Neuroscience Research*, 95(1–2), 291–300. <https://doi.org/10.1002/jnr.23884>
- Arnold, A. P., & Chen, X. (2009). What does the “four core genotypes” mouse model tell us about sex differences in the brain and other tissues? *Frontiers in Neuroendocrinology*, 30(1), 1–9. <https://doi.org/10.1016/j.yfrne.2008.11.001>
- Arnold, A. P., Chen, X., Grzybowski, M. N., Ryan, J. M., Sengelaub, D. R., Mohanroy, T., Furlan, V. A., Grisham, W., Malloy, L., Takizawa, A., Wiese, C. B., Vergnes, L., Skaletsky, H., Page, D. C., Reue, K., Harley, V. R., Dwinell, M. R., & Geurts, A. M. (2023). A “Four Core Genotypes” rat model to distinguish mechanisms underlying sex-biased phenotypes and diseases [Preprint]. *Genetics*. <https://doi.org/10.1101/2023.02.09.527738>
- Banakar, R., Eggenberger, A. L., Lee, K., Wright, D. A., Murugan, K., Zarecor, S., Lawrence-Dill, C. J., Sashital, D. G., & Wang, K. (2019). High-frequency random DNA insertions upon co-delivery of CRISPR-Cas9 ribonucleoprotein and selectable marker plasmid in rice. *Scientific Reports*, 9(1), 19902. <https://doi.org/10.1038/s41598-019-55681-y>
- Bridges, C. B. (1914). Direct Proof Through Non-Disjunction That the Sex-Linked Genes of *Drosophila* Are Borne by the X-Chromosome. *Science*, 40(1020), 107–109. <https://doi.org/10.1126/science.40.1020.107>

- Burgoyne, P. S., & Arnold, A. P. (2016). A primer on the use of mouse models for identifying direct sex chromosome effects that cause sex differences in non-gonadal tissues. *Biology of Sex Differences*, 7(1), 68. <https://doi.org/10.1186/s13293-016-0115-5>
- Charlesworth, B. (2003). The organization and evolution of the human Y chromosome. *Genome Biology*, 4(9), 226. <https://doi.org/10.1186/gb-2003-4-9-226>
- Cora, M. C., Kooistra, L., & Travlos, G. (2015). Vaginal Cytology of the Laboratory Rat and Mouse: Review and Criteria for the Staging of the Estrous Cycle Using Stained Vaginal Smears. *Toxicologic Pathology*, 43(6), 776–793.
<https://doi.org/10.1177/0192623315570339>
- Cyrus Chu, C. Y., & Lee, R. D. (2012). Sexual dimorphism and sexual selection: A unified economic analysis. *Theoretical Population Biology*, 82(4), 355–363.
<https://doi.org/10.1016/j.tpb.2012.06.002>
- Deng, W., Tsao, S. W., Lucas, J. N., Leung, C. S., & Cheung, A. L. M. (2003). A new method for improving metaphase chromosome spreading. *Cytometry*, 51A(1), 46–51.
<https://doi.org/10.1002/cyto.a.10004>
- Essers, J., De Stoppelaar, J. M., & Hoebee, B. (1995). A new rat repetitive DNA family shows preferential localization on chromosome 3, 12 and Y after fluorescence in situ hybridization and contains a subfamily which is Y chromosome specific. *Cytogenetic and Genome Research*, 69(3–4), 246–252. <https://doi.org/10.1159/000133974>
- Ford, C. (1959). A SEX-CHROMOSOME ANOMALY IN A CASE OF GONADAL DYSGENESIS (TURNER'S SYNDROME). *The Lancet*, 273(7075), 711–713.
[https://doi.org/10.1016/S0140-6736\(59\)91893-8](https://doi.org/10.1016/S0140-6736(59)91893-8)

- Goodfellow, P. N., & Lovell-Badge, R. (1993). *SRY AND SEX DETERMINATION IN MAMMALS*. *Annual Review of Genetics*, 27(1), 71–92.
<https://doi.org/10.1146/annurev.ge.27.120193.000443>
- Hamta, A., Adamovic, T., Samuelson, E., Helou, K., Behboudi, A., & Levan, G. (2006). Chromosome ideograms of the laboratory rat (*Rattus norvegicus*) based on high-resolution banding, and anchoring of the cytogenetic map to the DNA sequence by FISH in sample chromosomes. *Cytogenetic and Genome Research*, 115(2), 158–168.
<https://doi.org/10.1159/000095237>
- Henking, H. (1891). Spermatogenesis and its relationship to development in *Pyrrhocoris apterus* L. *Scientific Zool*, 51, 685–736.
- Howe, B., Umrigar, A., & Tsien, F. (2014). Chromosome preparation from cultured cells. *Journal of Visualized Experiments: JoVE*, 83, e50203. <https://doi.org/10.3791/50203>
- Jost, A. (1970). Hormonal factors in the sex differentiation of the mammalian foetus. *Philosophical Transactions of the Royal Society of London. Series B, Biological Sciences*, 259(828), 119–130. <https://doi.org/10.1098/rstb.1970.0052>
- Knufinke, M., MacArthur, M. R., Ewald, C. Y., & Mitchell, S. J. (2023). Sex differences in pharmacological interventions and their effects on lifespan and healthspan outcomes: A systematic review. *Frontiers in Aging*, 4, 1172789.
<https://doi.org/10.3389/fragi.2023.1172789>
- Link, J. C., Wiese, C. B., Chen, X., Avetisyan, R., Ronquillo, E., Ma, F., Guo, X., Yao, J., Allison, M., Chen, Y.-D. I., Rotter, J. I., El -Sayed Moustafa, J. S., Small, K. S., Iwase, S., Pellegrini, M., Vergnes, L., Arnold, A. P., & Reue, K. (2020). X chromosome dosage of

- histone demethylase KDM5C determines sex differences in adiposity. *Journal of Clinical Investigation*, 130(11), 5688–5702. <https://doi.org/10.1172/JCI140223>
- Lovell-Badge, R., & Robertson, E. (1990). XY female mice resulting from a heritable mutation in the primary testis determining gene, *Tdy*. *Development*, 109(3), 635–646. <https://doi.org/10.1242/dev.109.3.635>
- Mahadevaiah, S. K., Lovell-Badge, R., & Burgoyne, P. S. (1993). *Tdy*-negative XY, XXY and XYY female mice: Breeding data and synaptonemal complex analysis. *Reproduction*, 97(1), 151–160. <https://doi.org/10.1530/jrf.0.0970151>
- Markegard, C. B., Gallivan, C. P., Cheng, D. D., & Nguyen, H. D. (2016). Effects of Concentration and Temperature on DNA Hybridization by Two Closely Related Sequences via Large-Scale Coarse-Grained Simulations. *The Journal of Physical Chemistry B*, 120(32), 7795–7806. <https://doi.org/10.1021/acs.jpcc.6b03937>
- McCarthy, M. M., & Arnold, A. P. (2011). Reframing sexual differentiation of the brain. *Nature Neuroscience*, 14(6), 677–683. <https://doi.org/10.1038/nn.2834>
- McClung, C. E. (1899). A PECULIAR NUCLEAR ELEMENT IN THE MALE REPRODUCTIVE CELLS OF INSECTS. *Zoological Bulletin*, 2(4), 187–197. <https://doi.org/10.2307/1535425>
- Okomoda, V. T., Koh, I. C. C., Hassan, A., Amornsakun, T., Moh, J. H. Z., & Shahreza, S. M. (2018). Optimization of the cytogenetic protocol for *Pangasianodon hypophthalmus* (Sauvage, 1878) and *Clarias gariepinus* (Burchell, 1822). *PeerJ*, 6, e5712. <https://doi.org/10.7717/peerj.5712>
- Otto, S. (2008) *Sexual Reproduction and the Evolution of Sex*. *Nature Education* 1(1):182. (n.d.).

- Paliulis, L., Fabig, G., & Müller-Reichert, T. (2023). The X chromosome still has a lot to reveal – revisiting Hermann Henking’s work on firebugs. *Journal of Cell Science*, 136(4), jcs260998. <https://doi.org/10.1242/jcs.260998>
- Palmer, M. S., Berta, P., Sinclair, A. H., Pym, B., & Goodfellow, P. N. (1990). Comparison of human ZFY and ZFX transcripts. *Proceedings of the National Academy of Sciences*, 87(5), 1681–1685. <https://doi.org/10.1073/pnas.87.5.1681>
- Phoenix, C. H., Goy, R. W., Gerall, A. A., & Young, W. C. (1959). Organizing action of prenatally administered testosterone propionate on the tissues mediating mating behavior in the female guinea pig. *Endocrinology*, 65, 369–382. <https://doi.org/10.1210/endo-65-3-369>
- Piprek, R. P. (2020). History of The Research on Sex Determination. *Biomedical Journal of Scientific & Technical Research*, 25(3). <https://doi.org/10.26717/BJSTR.2020.25.004194>
- Plotton, I., Brosse, A., & Lejeune, H. (2010). Faut-il modifier la prise en charge du syndrome de Klinefelter pour améliorer les chances de paternité ? *Annales d'Endocrinologie*, 71(6), 494–504. <https://doi.org/10.1016/j.ando.2010.06.001>
- Ratcliffe, S. (1999). Long term outcome in children of sex chromosome abnormalities. *Archives of Disease in Childhood*, 80(2), 192–195. <https://doi.org/10.1136/adc.80.2.192>
- Ratcliffe, S. G., Bancroft, J., Axworthy, D., & McLaren, W. (1982). Klinefelter’s syndrome in adolescence. *Archives of Disease in Childhood*, 57(1), 6–12.
- Robertson, E., Bradley, A., Kuehn, M., & Evans, M. (1986). Germ-line transmission of genes introduced into cultured pluripotential cells by retroviral vector. *Nature*, 323(6087), 445–448. <https://doi.org/10.1038/323445a0>
- Simpson, J. L., De La Cruz, F., Swerdloff, R. S., Samango-Sprouse, C., Skakkebaek, N. E., Graham, J. M., Hassold, T., Aylstock, M., Meyer-Bahlburg, H. F. L., Willard, H. F., Hall, J.

- G., Salameh, W., Boone, K., Staessen, C., Geschwind, D., Giedd, J., Dobs, A. S., Rogol, A., Brinton, B., & Paulsen, C. A. (2003). Klinefelter syndrome: Expanding the phenotype and identifying new research directions. *Genetics in Medicine*, 5(6), 460–468.
<https://doi.org/10.1097/01.GIM.0000095626.54201.D0>
- Sinclair, A. H., Berta, P., Palmer, M. S., Hawkins, J. R., Griffiths, B. L., Smith, M. J., Foster, J. W., Frischauf, A.-M., Lovell-Badge, R., & Goodfellow, P. N. (1990). A gene from the human sex-determining region encodes a protein with homology to a conserved DNA-binding motif. *Nature*, 346(6281), 240–244. <https://doi.org/10.1038/346240a0>
- Smyth, C. M., & Bremner, W. J. (1998). Klinefelter Syndrome. *Archives of Internal Medicine*, 158(12), 1309. <https://doi.org/10.1001/archinte.158.12.1309>
- Tabata, J., Ichiki, R. T., Tanaka, H., & Kageyama, D. (2016). Sexual versus Asexual Reproduction: Distinct Outcomes in Relative Abundance of Parthenogenetic Mealybugs following Recent Colonization. *PloS One*, 11(6), e0156587.
<https://doi.org/10.1371/journal.pone.0156587>
- Tang, Y. Z., Gin, K. Y. H., & Lim, T. H. (2005). High-temperature fluorescent in situ hybridization for detecting *Escherichia coli* in seawater samples, using rRNA-targeted oligonucleotide probes and flow cytometry. *Applied and Environmental Microbiology*, 71(12), 8157–8164. <https://doi.org/10.1128/AEM.71.12.8157-8164.2005>
- Togashi, T., Bartelt, J. L., Yoshimura, J., Tainaka, K., & Cox, P. A. (2012). Evolutionary trajectories explain the diversified evolution of isogamy and anisogamy in marine green algae. *Proceedings of the National Academy of Sciences of the United States of America*, 109(34), 13692–13697. <https://doi.org/10.1073/pnas.1203495109>

- Turner, J. M. A., Mahadevaiah, S. K., Benavente, R., Offenberg, H. H., Heyting, C., & Burgoyne, P. S. (2000). Analysis of male meiotic “sex body” proteins during XY female meiosis provides new insights into their functions. *Chromosoma*, *109*(6), 426–432. <https://doi.org/10.1007/s004120000097>
- Van Der Heijden, G. W., Eijpe, M., & Baarends, W. M. (2011). The X and Y chromosome in meiosis: How and why they keep silent. *Asian Journal of Andrology*, *13*(6), 779–780. <https://doi.org/10.1038/aja.2011.93>
- Visootsak, J., & Graham, J. M. (2009a). Social function in multiple X and Y chromosome disorders: XXY, XYY, XXYY, XXXY. *Developmental Disabilities Research Reviews*, *15*(4), 328–332. <https://doi.org/10.1002/ddrr.76>
- Visootsak, J., & Graham, J. M. (2009b). Social function in multiple X and Y chromosome disorders: XXY, XYY, XXYY, XXXY. *Developmental Disabilities Research Reviews*, *15*(4), 328–332. <https://doi.org/10.1002/ddrr.76>
- Waldayer, H. (1888). About karyokinesis and its relationship to fertilization processes. *Microscopic Anatomy and Development Mechanics*, *32*, 1–122.
- Yang, R. K., Toruner, G. A., Wang, W., Fang, H., Issa, G. C., Wang, L., Quesada, A. E., Thakral, B., Patel, K. P., Peng, G., Liu, S., Yin, C. C., Borthakur, G., Tang, Z., Wang, S. A., Miranda, R. N., Khoury, J. D., Medeiros, L. J., & Tang, G. (2021). CBFβ Break-Apart FISH Testing: An Analysis of 1629 AML Cases with a Focus on Atypical Findings and Their Implications in Clinical Diagnosis and Management. *Cancers*, *13*(21), 5354. <https://doi.org/10.3390/cancers13215354>